

## Supporting Information

### **A Box-in-box Supramolecular Assembly for the Highly Selective Recognition of Natural, Epigenetically and Chemically Modified Nucleobases in Water**

Shu-Qin Qin<sup>a</sup>, Wei Xu<sup>a</sup>, Qi-Qi Wang<sup>a</sup>, Run-Yi Chen<sup>a</sup>, De-Zhi Yang<sup>b</sup>, Yang Lu<sup>b</sup>, Wen-Cai Ye<sup>a,c\*</sup>, Ren-Wang Jiang<sup>a,c\*</sup>

<sup>a</sup> State Key Laboratory of Bioactive Molecules and Druggability Assessment, College of Pharmacy, Jinan University, Guangzhou 510632, P. R. China.

<sup>b</sup> Institute of Materia Medica, Chinese Academy of Medical Sciences, 1 Xian Nong Tan Street, Beijing 100050, P. R. China.

<sup>c</sup> International Cooperative Laboratory of Traditional Chinese Medicine Modernization and Innovative Drug Development of Ministry of Education (MOE) of China, College of Pharmacy, Jinan University, Guangzhou 510632, P. R. China.

Correspondence:

e-mails: [trwjiang@jnu.edu.cn](mailto:trwjiang@jnu.edu.cn), [chywc@aliyun.com](mailto:chywc@aliyun.com)

Tel: 8620-85221016; Fax: 8620-85221559

## Table of contents

### S1. Synthesis and characterization of compounds

Figure S1a.  $^1\text{H}$  NMR spectrum of 2,6-dipyridyl phenylamine (400 MHz,  $\text{CDCl}_3$ )

Figure S1b.  $^{13}\text{C}$  NMR spectrum of 2,6-dipyridyl phenylamine (100 MHz,  $\text{CDCl}_3$ )

Figure S1c. ESI-TOF-MS spectrum of 2,6-dipyridyl phenylamine

Figure S1d.  $^1\text{H}$  NMR spectrum of  $\mathbf{1}\cdot(\text{Br})_4$  (400 MHz,  $\text{D}_2\text{O}$ )

Figure S1e.  $^{13}\text{C}$  NMR spectrum of  $\mathbf{1}\cdot(\text{Br})_4$  (100 MHz,  $\text{D}_2\text{O}$ )

Figure S1f. ESI-TOF-MS spectrum of  $\mathbf{1}\cdot(\text{Br})_4$

Figure S1g. ESI-TOF-MS spectrum of  $\mathbf{1}\cdot(\text{PF}_6)_4$

Scheme S1. Synthetic route to 2,6-dipyridyl phenylamine

Scheme S2. Synthetic route to  $\mathbf{1}\cdot(\text{PF}_6)_4$

### S2. Comparison of NMR spectra of the shiny particles and precipitate

Figure S2.  $^1\text{H}$ -NMR spectra of the shiny particles and precipitate

### S3. Crystal morphology and packing diagram of $\mathbf{1}^{4+}\cdot\text{SC4}^{4-}$ viewed down the $b$ -axis

Figure S3a. Crystal morphology

Figure S3b. Packing diagram of  $\mathbf{1}^{4+}\cdot\text{SC4}^{4-}$  viewed down the  $b$ -axis

### S4. IR Spectroscopies of $\mathbf{1}\cdot(\text{PF}_6)_4$ , SC4H and $\mathbf{1}^{4+}\cdot\text{SC4}^{4-}$

Figure S4. IR Spectroscopies of  $\mathbf{1}\cdot(\text{PF}_6)_4$ , SC4H and  $\mathbf{1}^{4+}\cdot\text{SC4}^{4-}$

### S5. Analysis of the molecular electrostatic potential (MEP) surface

Figure S5. MEPS of  $\mathbf{1}^{4+}\cdot\text{SC4}^{4-}$

### S6. NOESY spectroscopy of $\mathbf{1}^{4+}\cdot\text{SC4}^{4-}$

Figure S6. NOESY spectrum of  $\mathbf{1}^{4+}\cdot\text{SC4}^{4-}$  (400 MHz,  $\text{D}_2\text{O}$ ).

### S7. Precipitation of $\mathbf{1}^{4+}\cdot\text{SC4}^{4-}$ at $\text{pH} \geq 8$

Figure S7. pH responsive complexation of  $\mathbf{1}^{4+}\cdot\text{SC4}^{4-}$ . (a)  $\text{pH} = 8$ ; (b)  $\text{pH} = 10$ ;  
(c)  $\text{pH} = 12$ .

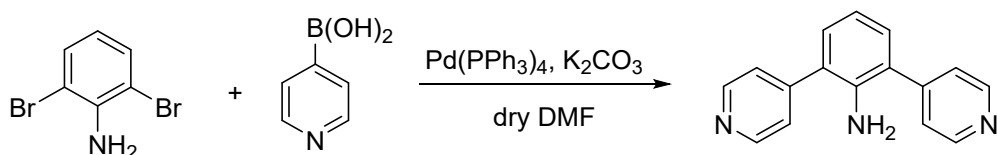
### S8. ITC analysis for epigenetically and chemically modified nucleobases with $\mathbf{1}^{4+}\cdot\text{SC4}^{4-}$

Figure S8. ITC thermogram and fitting from titrations of epigenetically and chemically modified nucleobases with  $\mathbf{1}^{4+}\cdot\text{SC4}^{4-}$ .

### S9. Crystal morphologies of $\mathbf{1}^{4+}\cdot\text{SC4}^{4-}@ \text{CTS}$ and $\mathbf{1}^{4+}\cdot\text{SC4}^{4-}@ \text{5F-CTS}$ and packing diagram viewed down the other directions.

Figure S9a. Pictures of crystals. (a)  $\mathbf{1}^{4+}\cdot\text{SC4}^{4-}@ \text{CTS}$ ; (b)  $\mathbf{1}^{4+}\cdot\text{SC4}^{4-}@ \text{CTS}$ .

- Figure S9b. Packing diagram of  $1^{4+}\cdot\text{SC}4^{4-}@$ CTS viewed down the *b*-axis
- Figure S9c. Packing diagram of  $1^{4+}\cdot\text{SC}4^{4-}@$ CTS viewed down the *c*-axis
- Figure S9d. Packing diagram of  $1^{4+}\cdot\text{SC}4^{4-}@$ 5F-CTS viewed down the *b*-axis
- S10. Guest volume calculations of CTS and 5F-CTS
- Fig. S10 Energy minimized structures of CTS (left) and 5F-CTS (right)
- S11. NOESY spectra of  $1^{4+}\cdot\text{SC}4^{4-}@$ CTS and  $1^{4+}\cdot\text{SC}4^{4-}@$ 5F-CTS
- Figure S11a. NOESY spectrum of  $1^{4+}\cdot\text{SC}4^{4-}@$ CTS (DMSO-*d*<sub>6</sub>).
- Figure S11b. NOESY spectrum of  $1^{4+}\cdot\text{SC}4^{4-}@$ 5F-CTS (DMSO-*d*<sub>6</sub>).
- S12. <sup>19</sup>F-NMR spectra of  $1^{4+}\cdot\text{SC}4^{4-}@$ 5F-CTS and 5F-CTS
- Figure S13. <sup>19</sup>F-NMR spectra of  $1^{4+}\cdot\text{SC}4^{4-}@$ 5F-CTS and 5F-CTS (DMSO-*d*<sub>6</sub>). (a)  $1^{4+}\cdot\text{SC}4^{4-}@$ 5F-CTS; (b) 5F-CTS
- S13. DFT calculations of the ternary complex of  $1^{4+}\cdot\text{SC}4^{4-}@$ CTS and  $1^{4+}\cdot\text{SC}4^{4-}@$ 5F-CTS
- Figure S13. DFT calculations of the ternary complex of  $1^{4+}\cdot\text{SC}4^{4-}@$ CTS and  $1^{4+}\cdot\text{SC}4^{4-}@$ 5F-CTS and binding energies
- S14. HPLC analyses of CTS and 5F-CTS in the precipitate and supernatant in *n*-butanol.
- Figure S14. HPLC chromatograms of CTS and 5F-CTS in the precipitate and supernatant fractions in *n*-butanol.
- Table S1. Experimental single crystal X-ray data of  $1^{4+}\cdot\text{SC}4^{4-}$ ,  $1^{4+}\cdot\text{SC}4^{4-}@$ CTS and  $1^{4+}\cdot\text{SC}4^{4-}@$ 5F-CTS.
- Table S2. Aromatic intermolecular interactions in Host and Guest
- Table S2a. C—H···π intermolecular interactions in Host and Guest
- Table S2b. π···π intermolecular interactions in Host and Guest
- Table S3. Hydrogen bonding intermolecular interactions in Host and Guest
- Table S4. <sup>1</sup>H-NMR shift changes after formation of  $1^{4+}\cdot\text{SC}4^{4-}$
- Table S5. <sup>1</sup>H-NMR shift changes after the formation of ternary complex  $1^{4+}\cdot\text{SC}4^{4-}@$ CTS
- Table S6. <sup>1</sup>H-NMR shift changes after the formation of ternary complex  $1^{4+}\cdot\text{SC}4^{4-}@$ 5F-CTS
- S1. Synthesis and characterization of the supramolecular salt ( $1^{4+}\cdot\text{SC}4^{4-}$ )**



Scheme S1. Synthetic route to 2,6-dipyridyl phenylamine

**1) Synthesis of compound 2,6-dipyridyl phenylamine.** **2,6-Dibromoaniline** (1 g, 3.98 mmol), 4-pyridineboronic acid (1.47 g, 11.96 mmol), Pd(PPh<sub>3</sub>)<sub>4</sub> (0.37 g, 0.32 mmol) and K<sub>2</sub>CO<sub>3</sub> (5.50 g, 39.8 mmol) were dissolved in dry DMF (100 mL). The mixed solution was stirred under N<sub>2</sub> atmosphere for 12 h at 120 °C. After cooling to room temperature, the mixture was extracted with CH<sub>2</sub>Cl<sub>2</sub> (3 × 30 mL), washed with H<sub>2</sub>O for three times, and dried over Na<sub>2</sub>SO<sub>4</sub>. It was further filtered and concentrated under reduced pressure and separated by silica gel column chromatography (CH<sub>2</sub>Cl<sub>2</sub>:MeOH=30:1) to afford **2,6-dipyridyl phenylamine** as a light yellow solid (735 mg, yield: 74.6%). <sup>1</sup>H NMR (400 MHz, CDCl<sub>3</sub>) δ 8.70 (d, *J* = 4.6 Hz, 4H, Ha), 7.45 (d, *J* = 4.6 Hz, 4H, Hb), 7.16 (d, *J* = 7.5 Hz, 2H, Hc), 6.94 (t, *J* = 7.4 Hz, 1H, Hd), 3.88 (s, 2H, He). <sup>13</sup>C NMR (100 MHz, CDCl<sub>3</sub>) δ 150.5 (Cg), 147.3 (Ce), 140.2 (Cd), 130.5 (Cb), 125.3 (Cf), 124.1 (Cc), 118.8 (Ca). ESI-TOF-MS: C<sub>16</sub>H<sub>13</sub>N<sub>3</sub> [M+H]<sup>+</sup> calcd. for 248.1109, found *m/z* 248.1180.

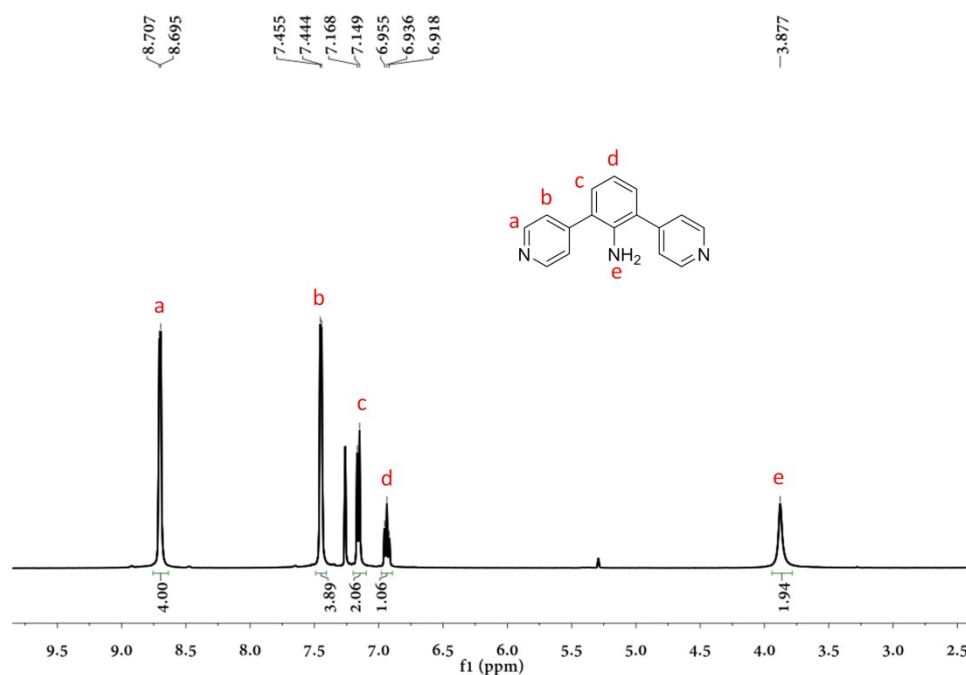


Figure S1a. <sup>1</sup>H NMR spectrum of 2,6-dipyridyl phenylamine (400 MHz, CDCl<sub>3</sub>)

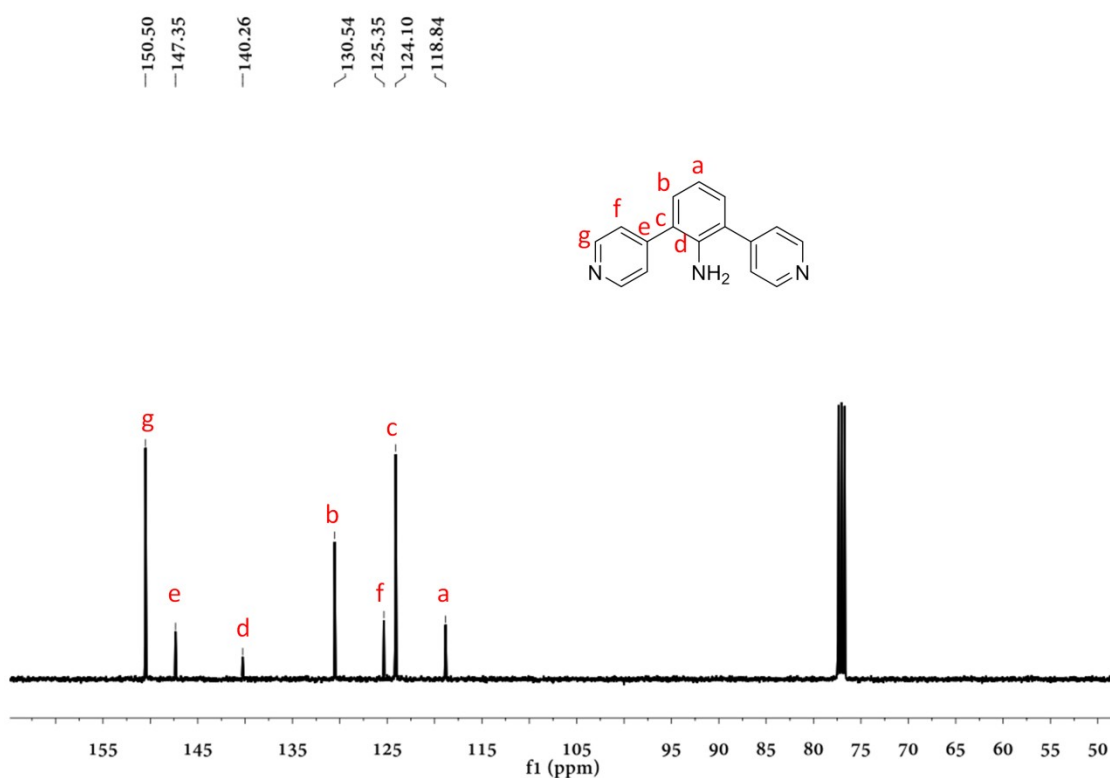


Figure S1b.  $^{13}\text{C}$  NMR spectrum of 2,6-dipyridyl phenylamine (100 MHz,  $\text{CDCl}_3$ )

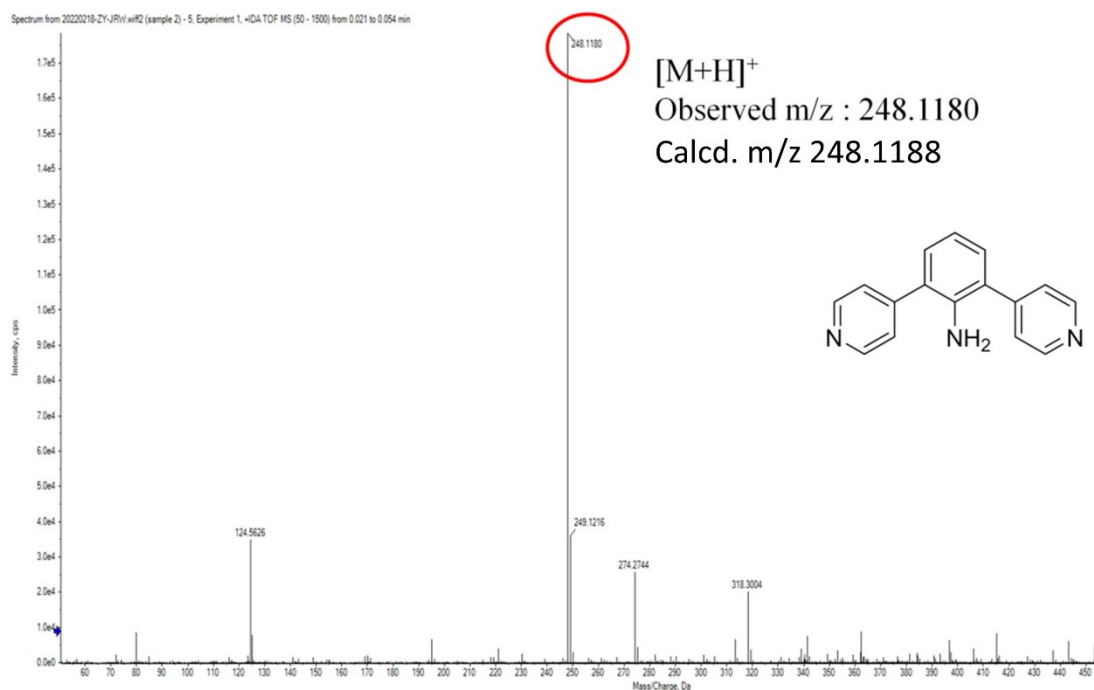
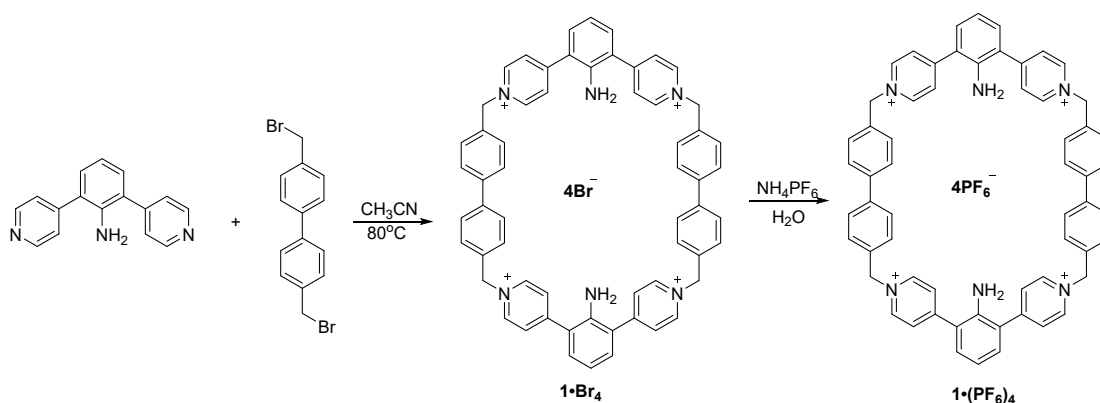


Figure S1c. ESI-TOF-MS spectrum of 2,6-dipyridyl phenylamine



Scheme S2. Synthetic route to **1·(PF<sub>6</sub>)<sub>4</sub>**

**2) Synthesis of compound 1.** The compound 2,6-dipyridyl phenylamine (500mg, 2.02 mmol) was dissolved in acetonitrile (200 mL), then 4,4'-bis(bromomethyl)biphenyl (687 mg, 2.02 mmol) was dissolved in acetonitrile (50 mL), and added slowly dropwise to the reaction flask with a dropping funnel, refluxed at 80 °C for 48 h, a large amount of yellow precipitate was produced. The reaction mixture was cooled to room temperature and the precipitate was washed three times with acetonitrile and dried under vacuum to obtain the compound **1·Br<sub>4</sub>** as a yellow solid (1161 mg, yield 48.9%). <sup>1</sup>H NMR (400 MHz, D<sub>2</sub>O) δ 8.97 (d, *J* = 6.8 Hz, 8H, Hd), 8.23 (d, *J* = 6.7 Hz, 8H, Hc), 7.78 (d, *J* = 8.2 Hz, 8H, Hf), 7.60 (d, *J* = 8.3 Hz, 8H, Hg), 7.49 (d, *J* = 7.8 Hz, 4H, Hb), 7.15 (s, 2H, Ha), 5.88 (s, 8H, He). <sup>13</sup>C NMR (100 MHz, D<sub>2</sub>O) 156.7 (Ce), 144.4 (Cg), 140.9 (Cd), 133.2 (Cl), 132.9 (Ci), 129.4 (Cj), 128.3 (Ck), 127.9 (Cf), 124.5 (Cb), 123.1 (Ca), 115.0 (Cc), 63.8 (Ch). ESI-TOF-MS: C<sub>60</sub>H<sub>51</sub>N<sub>6</sub>Br<sub>4</sub> [M+H]<sup>+</sup> calcd. for 1171.0909, found *m/z* 1171.0918.

### 3) Counterion exchange

The **1·Br<sub>4</sub>** (200 mg, 0.17 mmol) was dissolved in H<sub>2</sub>O (500 mL), NH<sub>4</sub>PF<sub>6</sub> was added in the solution. The solution was stirred until the precipitate was not formed anymore. Then, the precipitate was collected through the filtration. The precipitate was washed three times with H<sub>2</sub>O and dried under vacuum to obtain the compound **1·(PF<sub>6</sub>)<sub>4</sub>** as a yellow solid (194 mg, yield 79.6%). ESI-TOF-MS: C<sub>60</sub>H<sub>50</sub>N<sub>6</sub>(PF<sub>6</sub>)<sub>4</sub> [M+H]<sup>+</sup> calcd. for 1435.2742, found *m/z* 1435.2740.

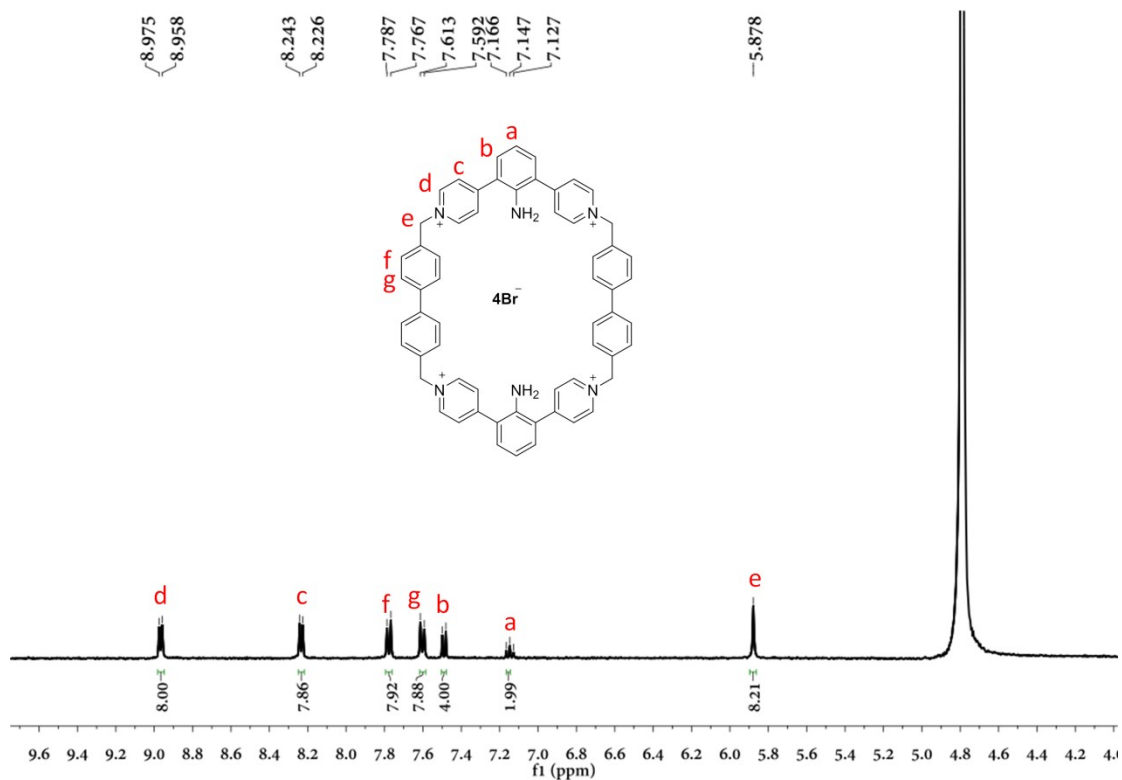


Figure S1d.  $^1\text{H}$  NMR spectrum of  $1 \cdot (\text{Br})_4$  (400 MHz,  $\text{D}_2\text{O}$ )

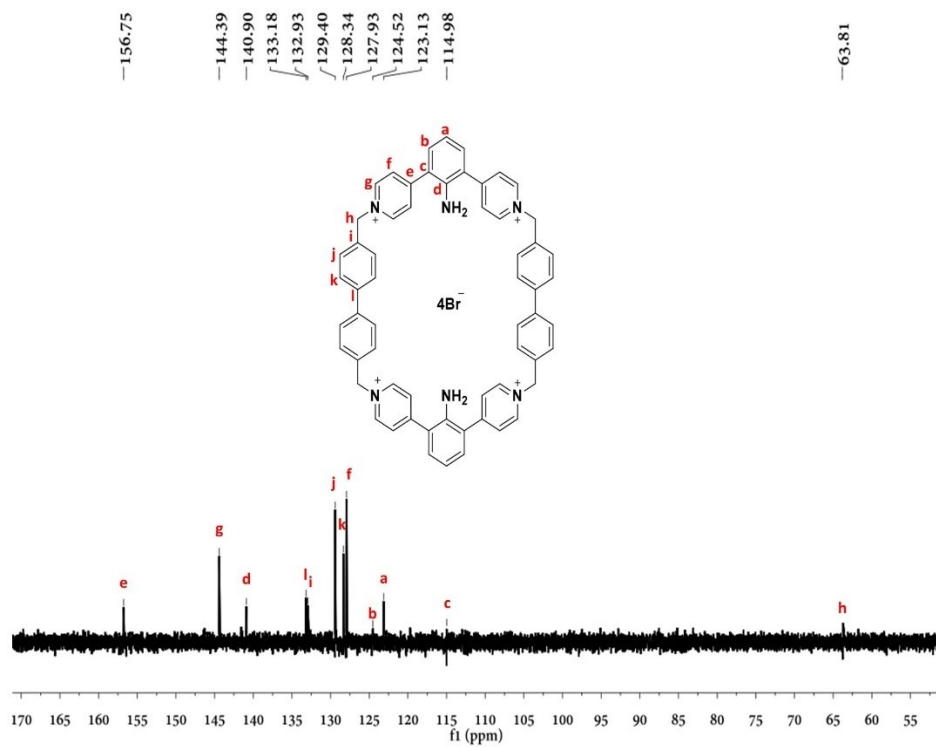


Figure S1e.  $^{13}\text{C}$  NMR spectrum of  $1 \cdot (\text{Br})_4$  (100 MHz,  $\text{D}_2\text{O}$ )

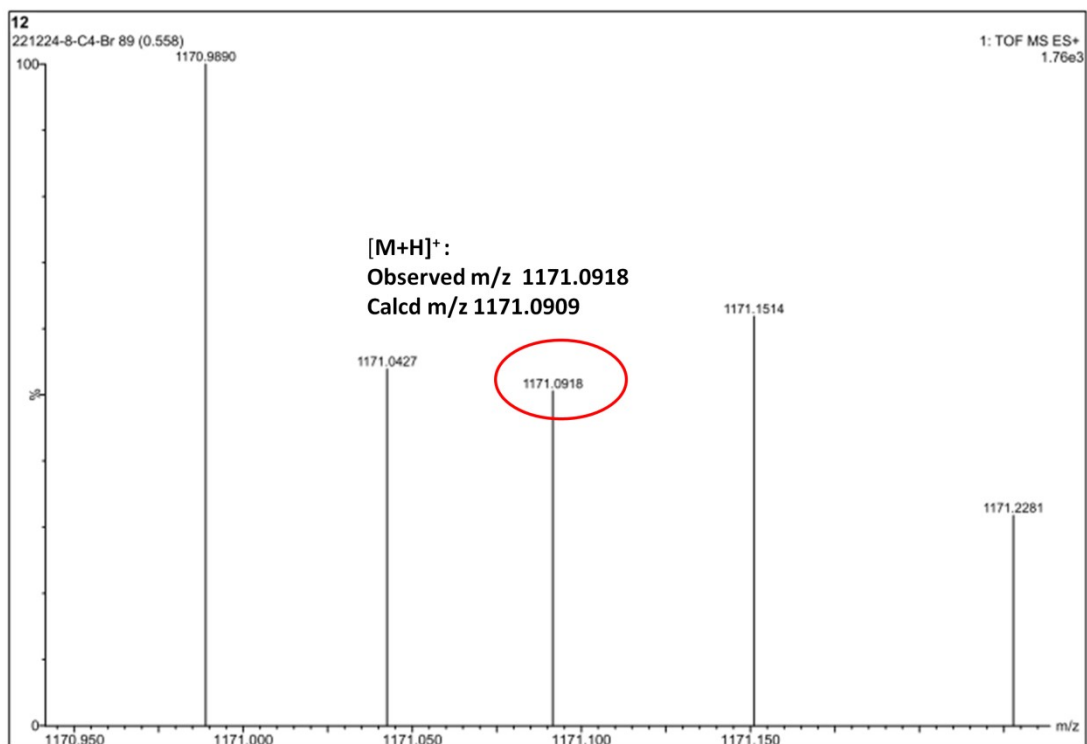


Figure S1f. ESI-TOF-MS spectrum of  $1 \cdot (\text{Br})_4$

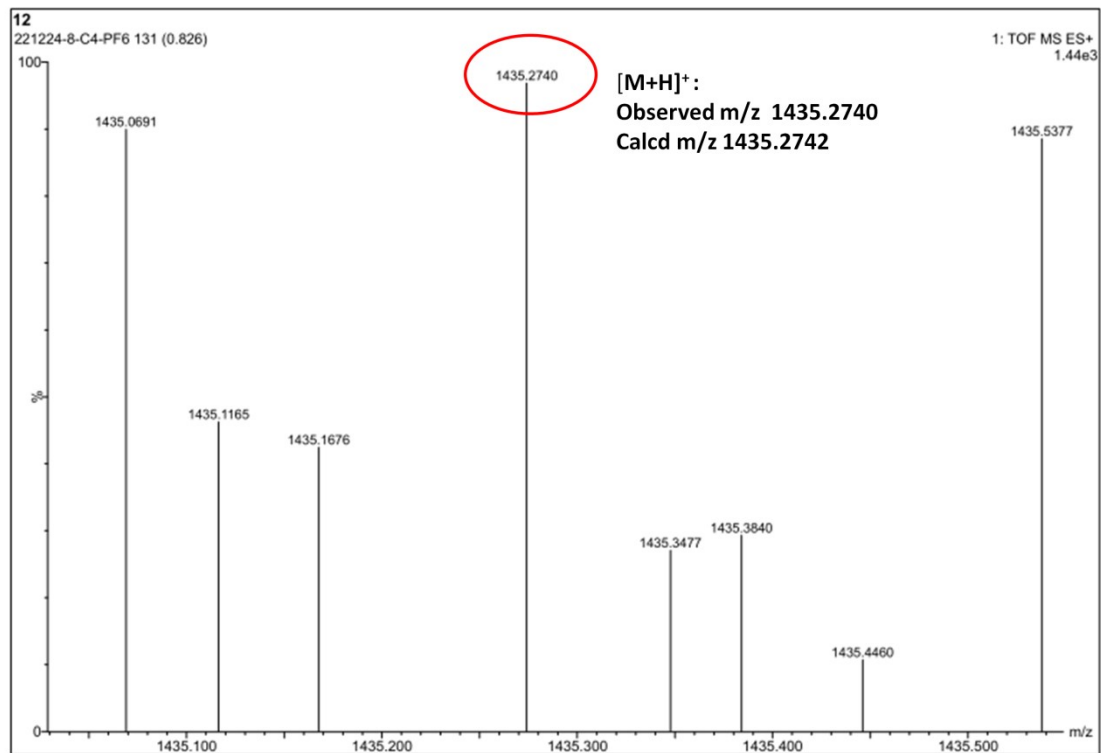


Figure S1g. ESI-TOF-MS spectrum of  $1 \cdot (\text{PF}_6)_4$



## S2. Comparison of $^1\text{H-NMR}$ spectra of the shiny particles and precipitate

When mixed high concentrations ( $\geq 40 \mu\text{M}$ ) of  $\mathbf{1}\cdot(\text{PF}_6)_4$  and  $\text{SC4H}$  (1:1), the precipitate would be firstly observed followed by some shiny particles. We compared the precipitate and the shiny particles by  $^1\text{H-NMR}$  which showed that they shared the same composition (Fig. S2).

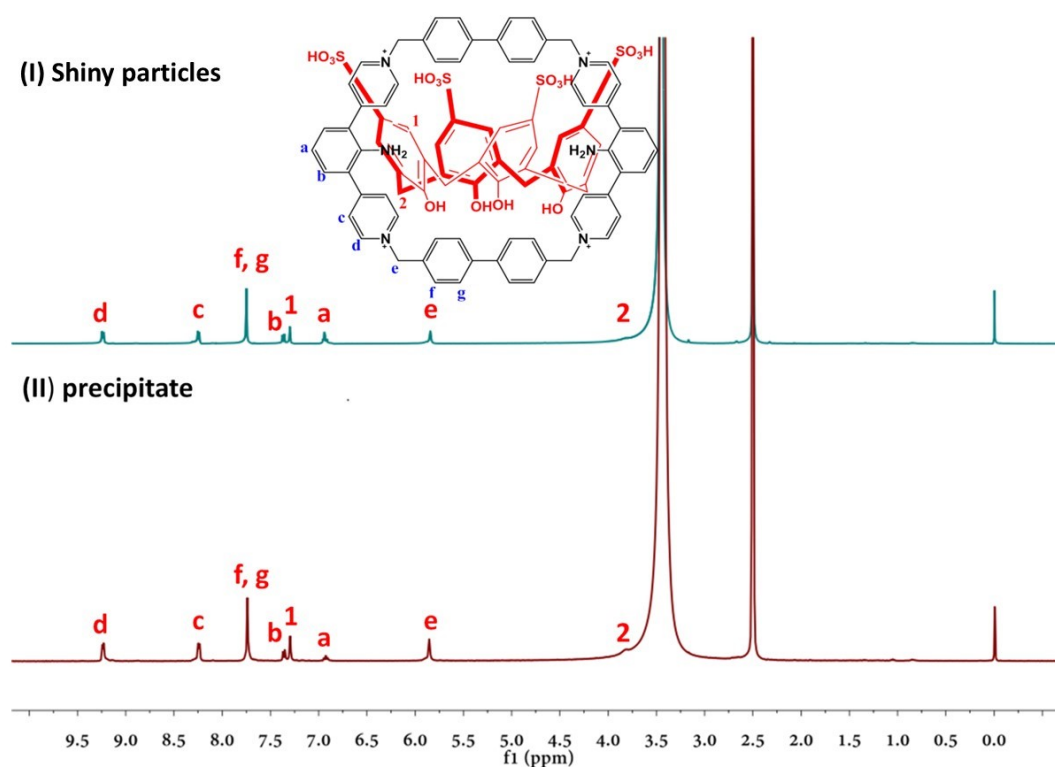


Figure S2.  $^1\text{H-NMR}$  spectra of the shiny particles and precipitate

## S3 Crystal morphology and packing diagram of $\mathbf{1}^{4+}\cdot\text{SC4}^{4-}$ viewed down the $b$ -axis

The crystals of  $\mathbf{1}^{4+}\cdot\text{SC4}^{4-}$  were observed by a Mshot MZ62 microscope, and the crystal morphology was shown in Figure 3a. The packing diagram of  $\mathbf{1}^{4+}\cdot\text{SC4}^{4-}$  viewed down the  $b$ -axis was drawn by Diamond software and was shown in Figure S3b.

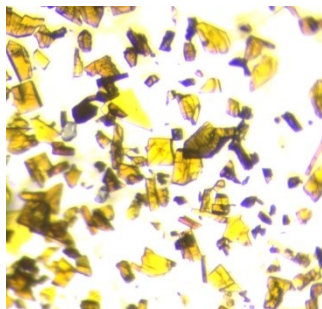


Figure S3a. Crystal morphology of  $1^{4+}·SC4^{4-}$

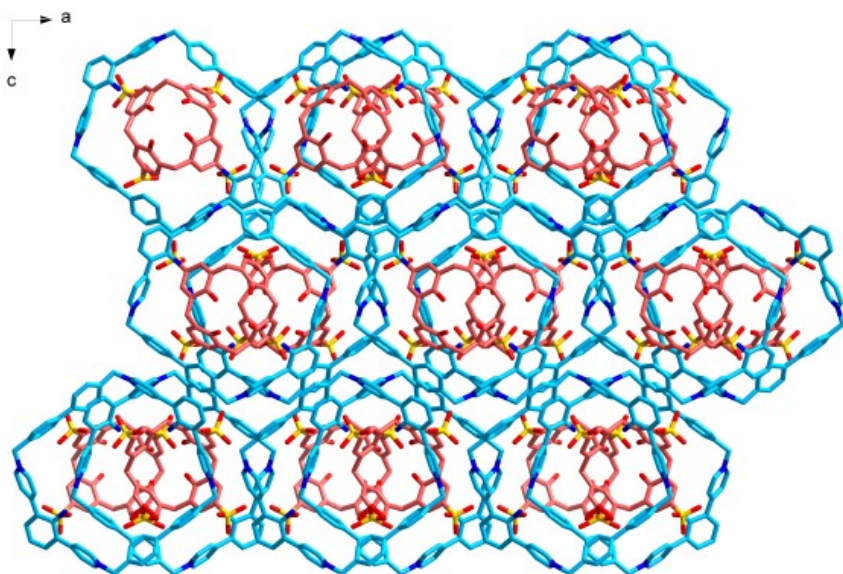


Figure S3b. Packing diagram of  $1^{4+}·SC4^{4-}$  viewed down the  $b$ -axis

#### S4. IR Spectroscopies of $1·(PF_6)_4$ , SC4H and $1^{4+}·SC4^{4-}$ .

IR spectra were obtained utilizing an FT/IR-4600 spectrometer. IR Spectroscopies of  $1·(PF_6)_4$ , SC4H and  $1^{4+}·SC4^{4-}$  was shown in Figure S4.

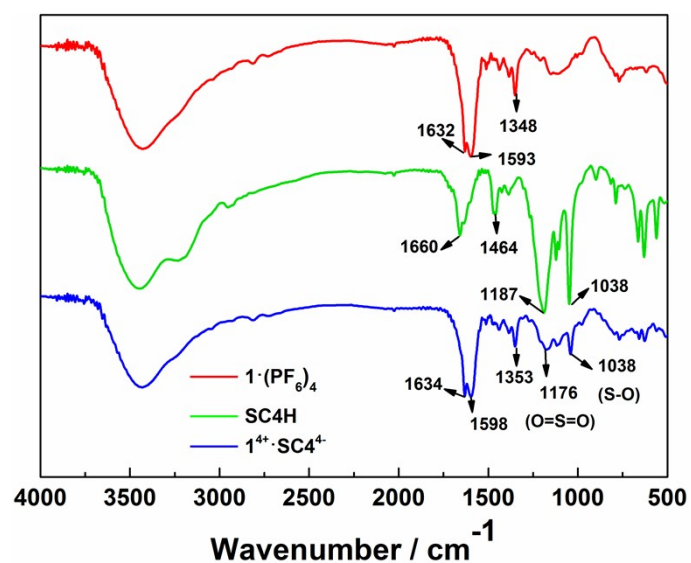


Figure S4. IR Spectroscopies of  $1 \cdot (\text{PF}_6)_4$ ,  $\text{SC}_4\text{H}$  and  $1^{4+} \cdot \text{SC}_4^{4-}$ .

### S5 Analysis of the molecular electrostatic potential (MEP) surface

The molecular electrostatic potential (MEP) on the molecular surface is critical for understanding and predicting intermolecular interaction. The ESPs mapped on  $1^{4+}$  and  $\text{SC}_4^{4-}$  are shown in Figure S42, in which red represents positive potential while blue represents negative potential. As a result,  $1^{4+}$  and  $\text{SC}_4^{4-}$  forms a salt.

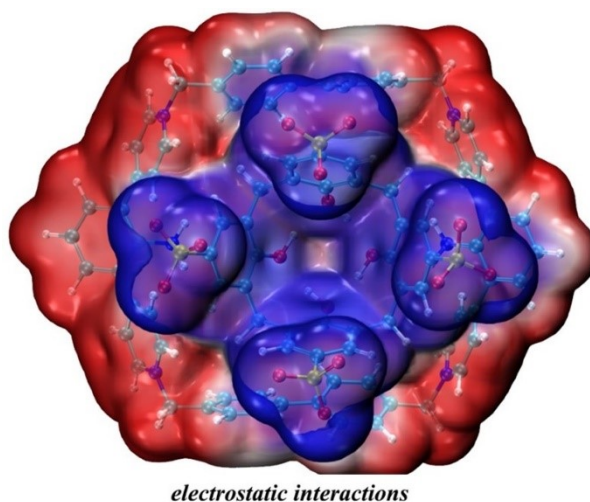


Figure S5. MEPS of  $1^{4+} \cdot \text{SC}_4^{4-}$

### S6. NOESY spectroscopy of $1^{4+} \cdot \text{SC}_4^{4-}$

<sup>1</sup>H-<sup>1</sup>H NOESY spectra were recorded on a Bruker Avance-400 NMR spectrometer.

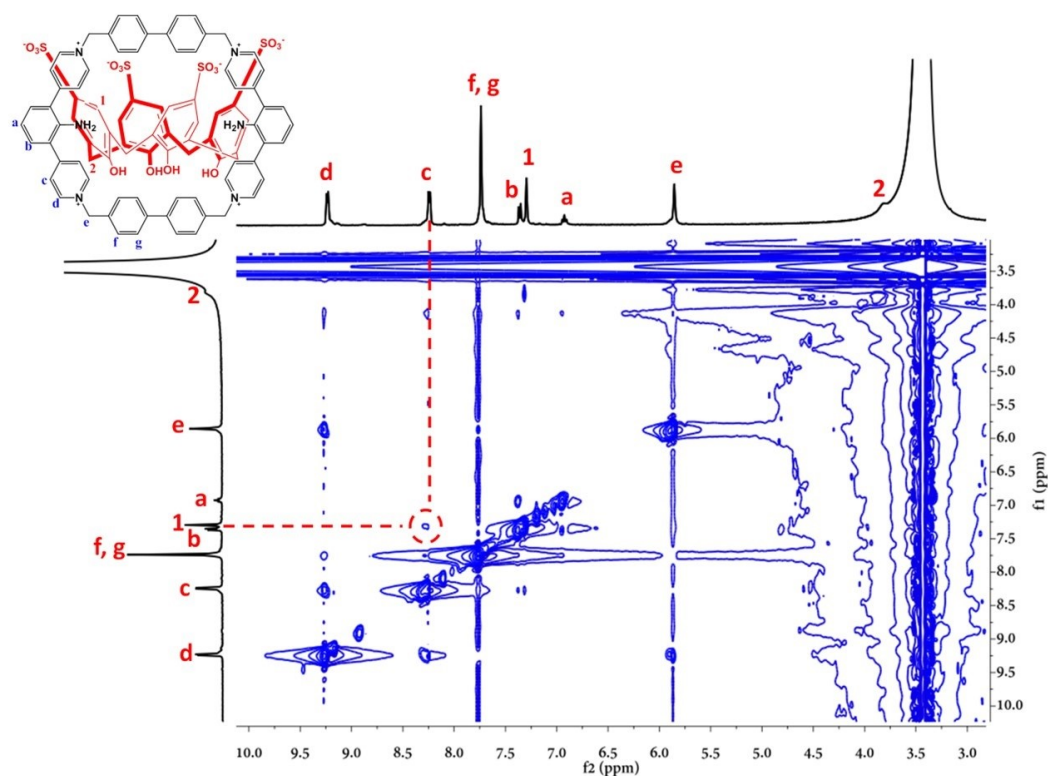


Figure S6. NOESY spectrum of  $1^{4+} \cdot SC4^{4-}$  (400 MHz,  $D_2O$ ).

### S7. Precipitation of $1^{4+} \cdot SC4^{4-}$ at $pH \geq 8$

$1^{4+} \cdot SC4^{4-}$  was stable at neutral condition. However, it would be destroyed at pH value higher than 8. Thus, formation of supramolecular salt  $1^{4+} \cdot SC4^{4-}$  was pH responsive.

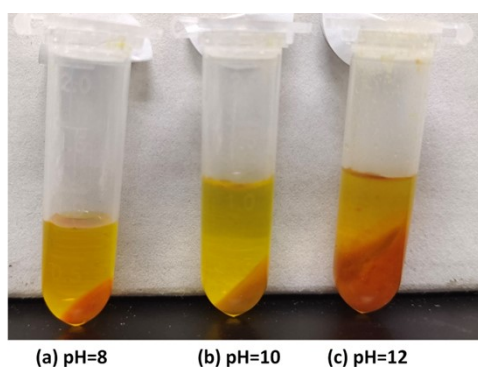


Figure S7. pH responsive complexation of  $1^{4+} \cdot SC4^{4-}$ . (a)  $pH=8$ ; (b)  $pH=10$ ;  
(c)  $pH=12$ .

### S8 ITC analysis for epigenetically and chemically modified nucleobases with $1^{4+} \cdot SC4^{4-}$

Isothermal Titration Calorimetry (ITC) experiments were carried out in deionized

water at 25 °C on a Malvern/Micro PEAQ-ITC Automated instrument for three times. The stirring rate is 250 r/min with titration in every 250 seconds (10  $\mu$ L each time). Altogether, 19 consecutive titrations were performed. The data was fitted using the instrument software (MicroCal PEAQ ITC Analyze).

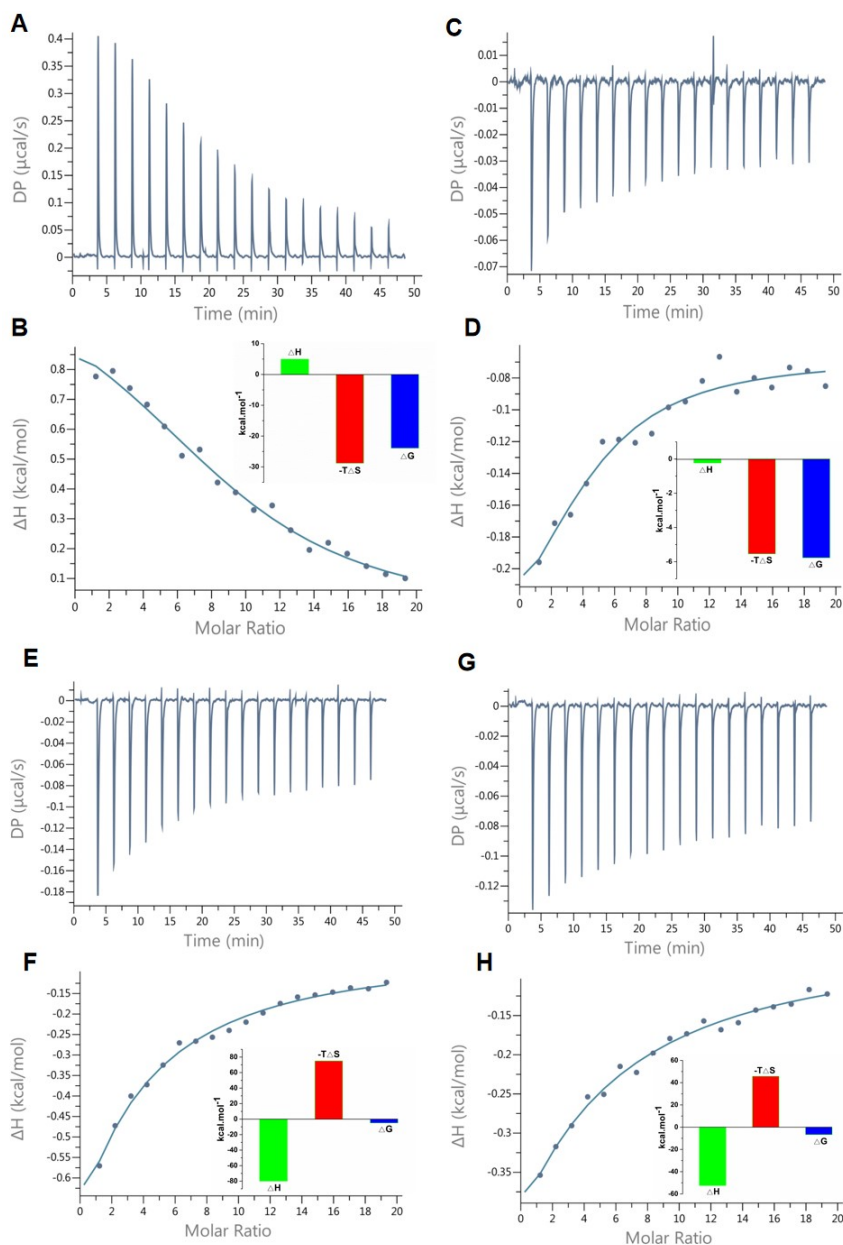


Figure S8. ITC thermogram and fitting from titrations of epigenetically and chemically modified nucleobases with  $1^{4+}$ .SC4<sup>4-</sup>. A: ITC thermogram resulting from titrations of 5-methylcytosine with  $1^{4+}$ .SC4<sup>4-</sup>; B: fitting the thermogram Figure 8A with a single site model; C: ITC thermogram resulting from titrations of 5-hydroxymethylcytosine with  $1^{4+}$ .SC4<sup>4-</sup>; D: fitting the thermogram Figure 8C with a single site model; E: ITC thermogram resulting from titrations of cytarabine with  $1^{4+}$ .SC4<sup>4-</sup>; F: fitting the thermogram Figure 8E with a single site model; G: ITC thermogram resulting from titrations of gemcitabine with  $1^{4+}$ .SC4<sup>4-</sup>; H: fitting the thermogram Figure 8G with a single site model.

S9 Crystal morphologies of  $1^{4+}\cdot\text{SC4}^{4+}\text{@CTS}$  and  $1^{4+}\cdot\text{SC4}^{4+}\text{@5F-CTS}$  and packing diagram viewed down the other directions.

The crystals of  $1^{4+}\cdot\text{SC4}^{4+}\text{@CTS}$  and  $1^{4+}\cdot\text{SC4}^{4+}\text{@5F-CTS}$  were observed by a Mshot MZ62 microscope, and the crystal morphologies were shown in Figure 9a. The packing diagram of  $1^{4+}\cdot\text{SC4}^{4+}\text{@CTS}$  and  $1^{4+}\cdot\text{SC4}^{4+}\text{@5F-CTS}$  viewed down the other directions were drawn by Diamond software (Figures S9b, S9c and S9d).

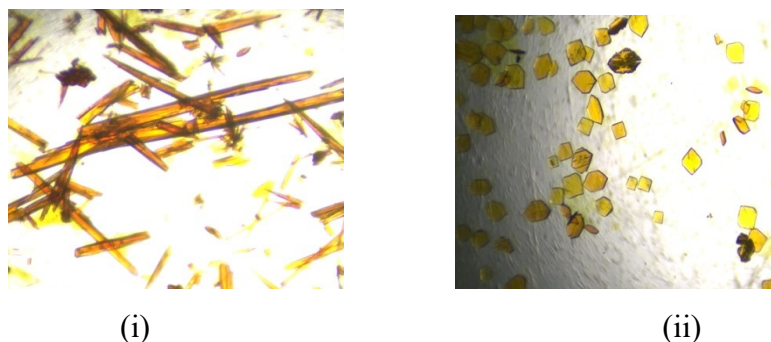


Figure S9a. Pictures of crystals. (i)  $1^{4+}\cdot\text{SC4}^{4+}\text{@CTS}$ ; (ii)  $1^{4+}\cdot\text{SC4}^{4+}\text{@5F-CTS}$ .

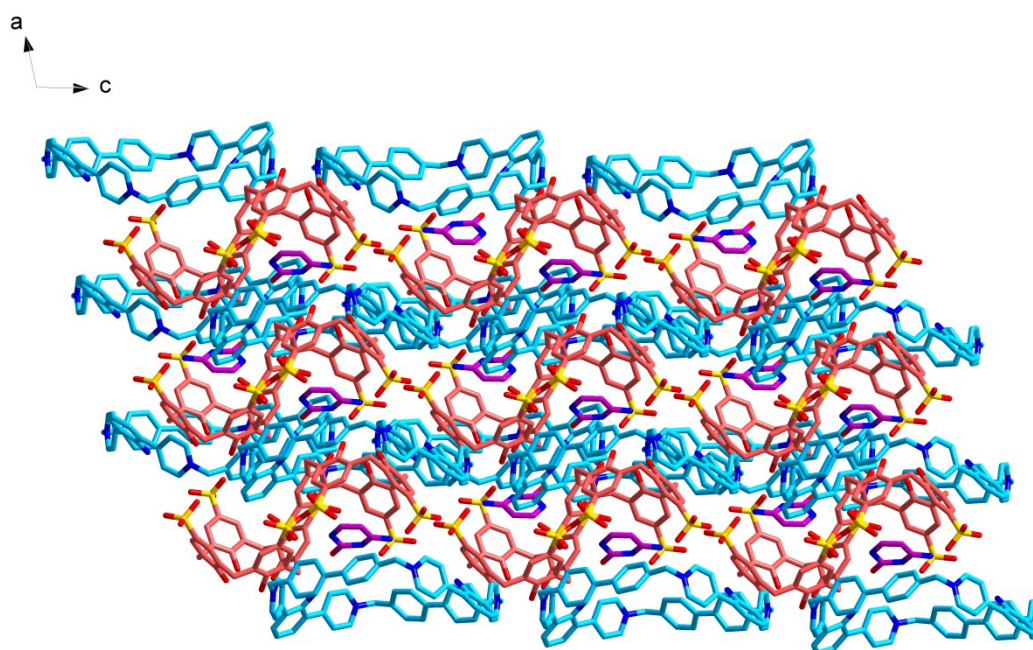


Figure S9b. Packing diagram of  $1^{4+}\cdot\text{SC4}^{4+}\text{@CTS}$  viewed down the *b*-axis

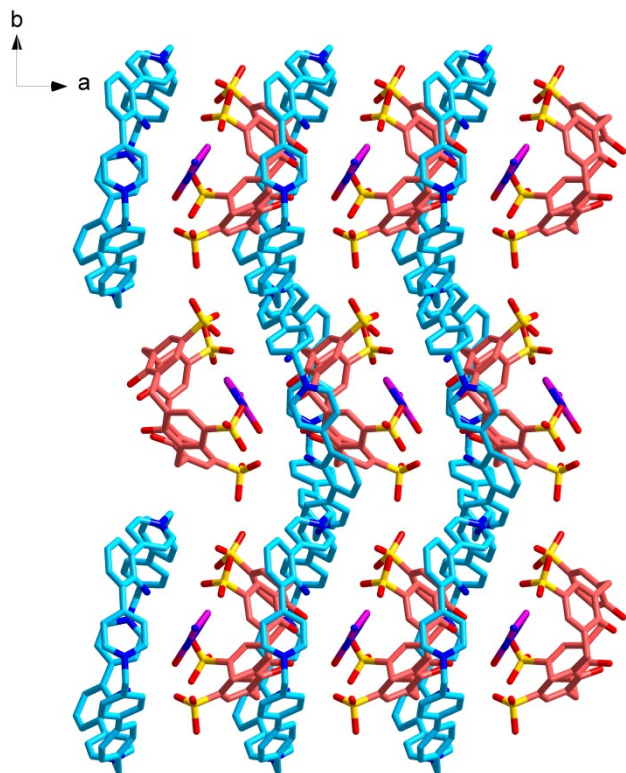


Figure S9c. Packing diagram of  $1^{4+} \cdot SC4^{4+} @ CTS$  viewed down the *c*-axis

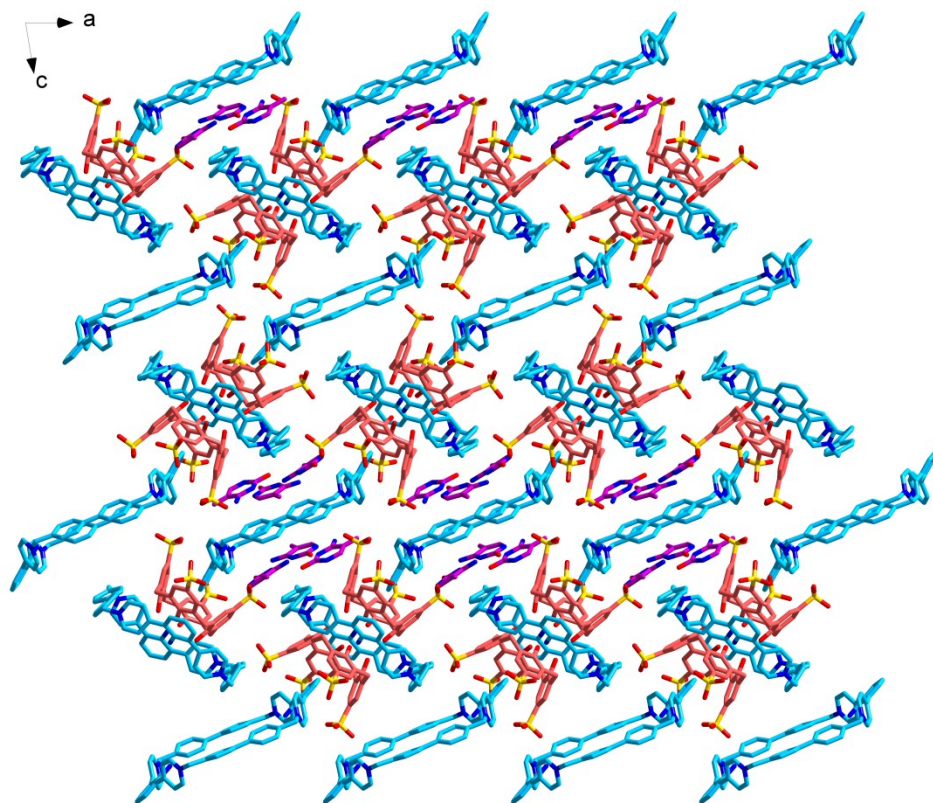


Figure S9d. Packing diagram of  $1^{4+} \cdot SC4^{4+} @ 5F-CTS$  viewed down the *b*-axis

## S10 Guest volume calculations of CTS and 5F-CTS

The guest structures were drawn by Chemdraw. Then, the structures were imported into Chem3D, and performed minimum energy optimization. The volume of guests were performed at 6-311++G(d,p) level using the Gaussian 09 program. The length and width of the guests and host are measured by diamond.

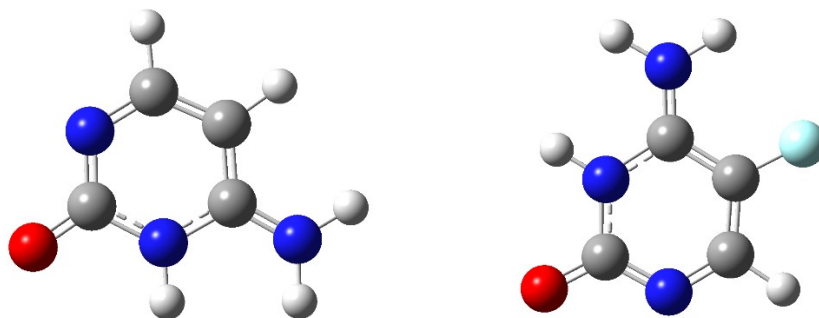


Fig. S10 Energy minimized structures of CTS (left) and 5F-CTS (right)

### Cartesian coordinates (Å) for the optimized geometries of CTS

C	-0.63780000	0.46110000	0.60380000
C	0.55280000	0.90390000	1.03170000
C	1.65290000	0.44360000	0.41190000
N	1.64960000	-0.38040000	-0.54990000
C	0.54960000	-0.83300000	-0.99560000
N	-0.60480000	-0.41100000	-0.41690000
O	0.47260000	-1.62190000	-1.91040000
N	-1.73500000	0.82710000	1.11320000
H	0.63310000	1.62190000	1.86390000
H	2.64730000	0.79040000	0.74200000
H	-1.49420000	-0.74770000	-0.74350000
H	-1.74420000	1.50910000	1.91040000
H	-2.64730000	0.45730000	0.74950000

### Cartesian coordinates (Å) for the optimized geometries of 5F-CTS

C	-0.63610000	0.38530000	0.53880000
---	-------------	------------	------------



C	0.55440000	0.83120000	0.97640000
C	1.65320000	0.36820000	0.35320000
N	1.65040000	-0.45330000	-0.61140000
C	0.55250000	-0.90530000	-1.06280000
N	-0.60270000	-0.48420000	-0.48480000
O	0.47770000	-1.69160000	-1.98050000
N	-1.73180000	0.75280000	1.04950000
F	0.64700000	1.69160000	1.98050000
H	2.64760000	0.71190000	0.68510000
H	-1.49180000	-0.81900000	-0.81380000
H	-1.72830000	1.43320000	1.84850000
H	-2.64760000	0.38930000	0.68890000

### S11. NOESY spectra of $1^{4+} \cdot \text{SC4}^{4-} @ \text{CTS}$ and $1^{4+} \cdot \text{SC4}^{4-} @ 5\text{F-CTS}$

$^1\text{H}$ - $^1\text{H}$  NOESY spectra of  $1^{4+} \cdot \text{SC4}^{4-} @ \text{CTS}$  and  $1^{4+} \cdot \text{SC4}^{4-} @ 5\text{F-CTS}$  were recorded on a Bruker Avance-400 NMR spectrometer.

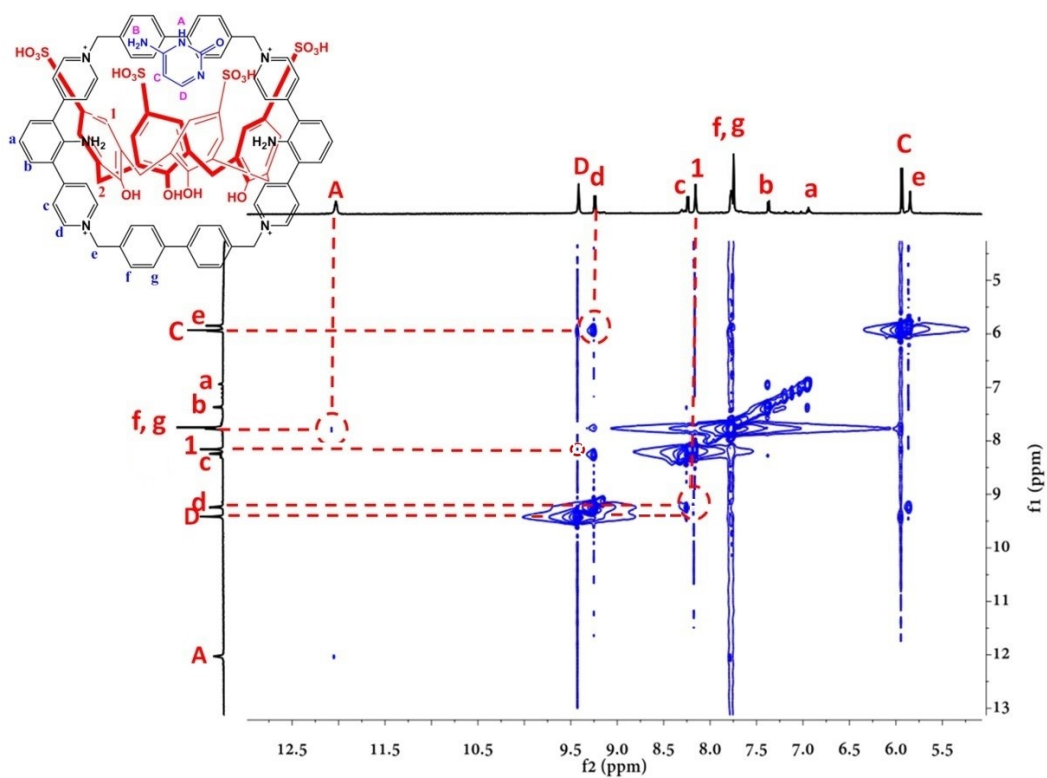


Figure S11a. NOESY spectrum of  $1^{4+} \cdot \text{SC4}^{4-} @ \text{CTS}$  ( $\text{DMSO-}d_6$ ).

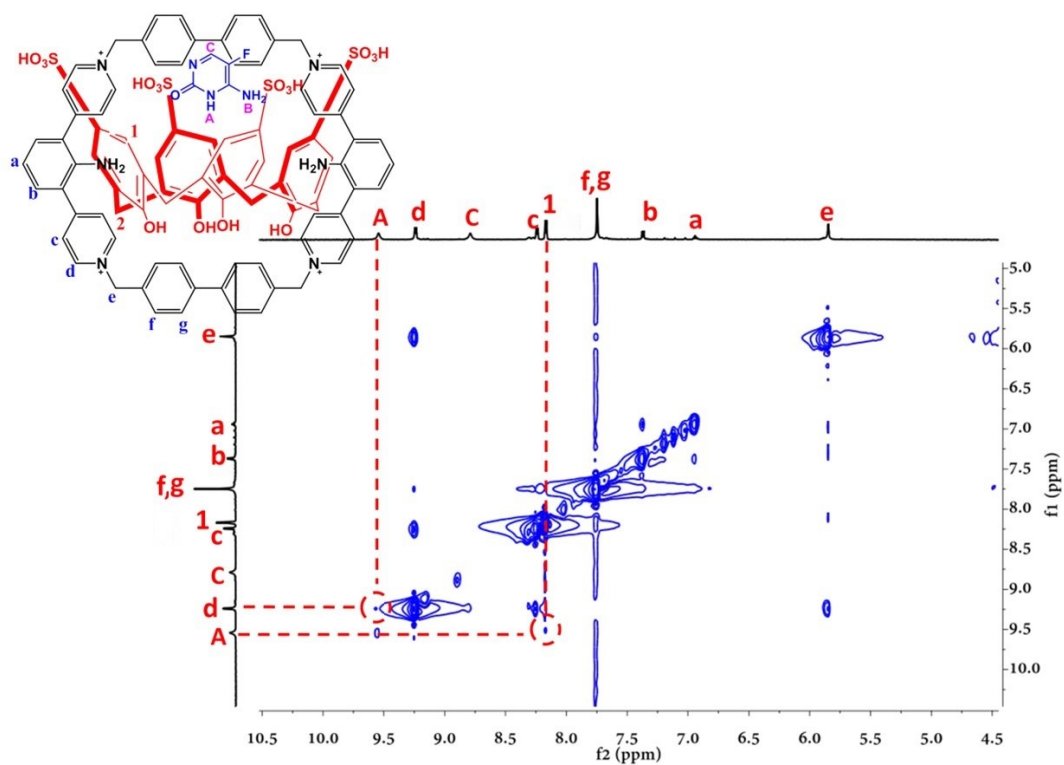


Figure S11b. NOESY spectrum of  $1^{4+}\cdot\text{SC4}^{4+}@5\text{F-CTS}$  ( $\text{DMSO-}d_6$ ).

### S12. $^{19}\text{F}$ -NMR spectra of $1^{4+}\cdot\text{SC4}^{4+}@5\text{F-CTS}$ and 5F-CTS

$^{19}\text{F}$ -NOESY spectra of  $1^{4+}\cdot\text{SC4}^{4+}@5\text{F-CTS}$  and 5F-CTS were recorded on a Bruker Avance-400 NMR spectrometer.

(a)  $1^{4+}\cdot\text{SC4}^{4+}@5\text{F-CTS}$

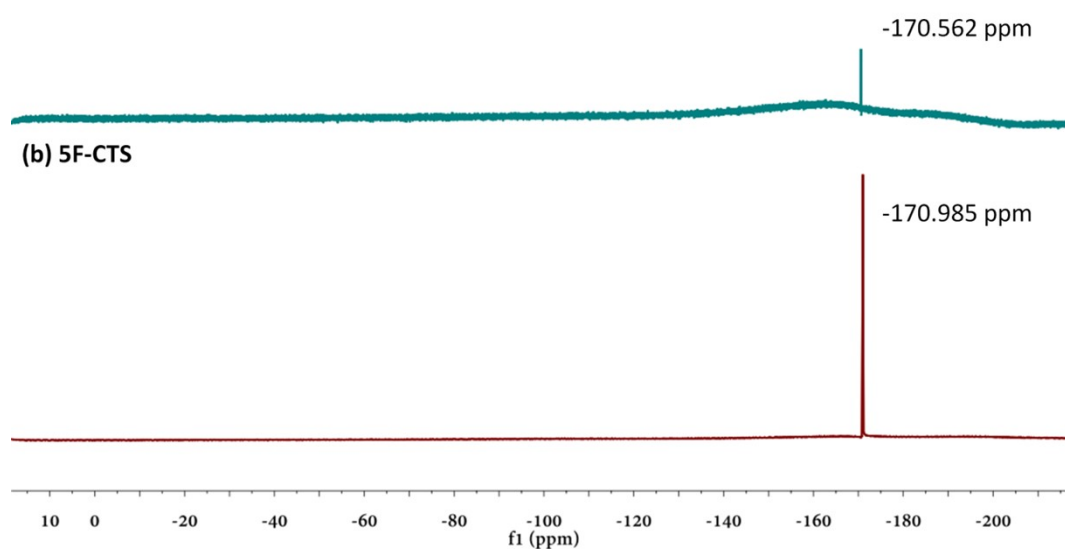


Figure S12.  $^{19}\text{F}$ -NMR spectra of  $1^{4+}\cdot\text{SC4}^{4+}@5\text{F-CTS}$  and 5F-CTS ( $\text{DMSO-}d_6$ ). (a)  $1^{4+}\cdot\text{SC4}^{4+}@5\text{F-CTS}$ ; (b) 5F-CTS

**S13** DFT calculations of the ternary complexes of  $1^{4+} \cdot SC4^{4-} @ CTS$  and  $1^{4+} \cdot SC4^{4-} @ 5F-CTS$

All calculations were carried out using the Gaussian 09 program<sup>s1</sup>. All structures were fully optimized at B3LYP/6-31G(d)<sup>s2</sup> theoretical level in water ( $\epsilon=5.6968$ ) using the SMD method of Truhlar and Cramer<sup>s3</sup>. The initial structures for complex are prepared based on the X-ray structures. The total electron energies are used to calculate the binding energies.

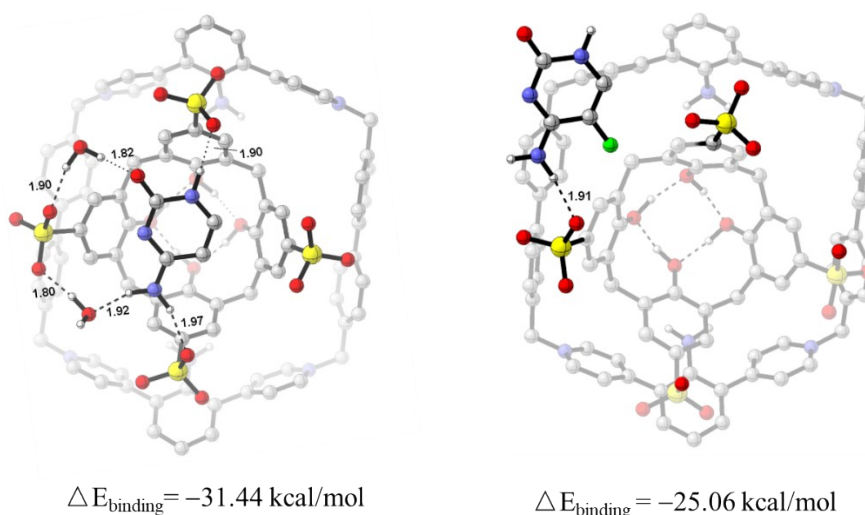


Figure S13. DFT calculations of the ternary complex of  $1^{4+} \cdot SC4^{4-} @ CTS$  and  $1^{4+} \cdot SC4^{4-} @ 5F-CTS$  and binding energies

**Energy calculations**

B3LYP/6-31G(d) Cartesian coordinates and energies in Hartree

**Cytosine (CTS)**

N	7.76805	18.3818	14.31538
O	7.80805	17.5138	16.42038
C	6.53005	20.5458	14.34438
H	6.17405	21.3368	13.95338
C	7.42805	18.4198	15.64338
N	6.70405	19.3998	16.27338
C	7.41905	19.5608	13.48838
N	7.95505	19.3668	12.32938
H	8.41905	18.6368	12.17638

H	7.85605	19.9678	11.69338
C	6.31005	20.2818	15.50438
H	5.70005	20.8828	15.91238
H	6.51466	19.39991	17.25528

B3LYP/6-31G(d) Total Energy: -394.9278499

**5F-Cytosine (5F-CTS)**

N	7.76805	18.3818	14.31538
O	7.80805	17.5138	16.42038
C	6.53005	20.5458	14.34438
C	7.42805	18.4198	15.64338
N	6.70405	19.3998	16.27338
C	7.41905	19.5608	13.48838
N	7.95505	19.3668	12.32938
H	8.41905	18.6368	12.17638
H	7.85605	19.9678	11.69338
C	6.31005	20.2818	15.50438
H	5.70005	20.8828	15.91238
H	6.51466	19.39991	17.25528
F	6.02494	21.66812	13.78961

B3LYP/6-31G(d) Total Energy: -494.1521395

**Complex 1 (1<sup>4+</sup>.SC4<sup>4+</sup>@CTS)**

S	4.542	23.492	16.909
S	5.565	17.257	19.344
S	6.693	21.869	10.096
S	7.919	14.661	12.28
O	0.761	19.821	14.262
H	1.041	19.589	13.503
O	5.074	22.785	18.065
O	4.901	17.449	20.621
O	1.91	19.04	12.008
H	2.1474	18.29792	12.3237
O	3.743	24.662	17.308
O	1.347	17.102	15.25
H	1.17266	17.87396	14.96989

O	5.555	23.846	15.949
O	2.479	16.747	12.953
H	2.33026	16.89413	13.76755
O	6.381	23.249	9.767
O	7.163	21.172	8.908
O	6.35	16.062	19.278
O	7.62	21.75	11.225
O	6.344	18.453	19.01
C	2.37	18.158	17.089
O	8.366	14.99	10.96
C	2.388	17.162	16.128
C	2.262	21.649	14.117
C	2.864	21.344	16.812
H	3.068	21.244	17.735
C	3.969	19.007	10.828
C	4.489	16.674	11.661
C	1.96	20.454	16.215
C	3.17	22.506	14.761
H	3.591	23.2	14.268
C	3.761	16.338	12.794
C	3.13	21.068	11.813
C	1.68	20.631	14.857
C	3.88	17.522	10.555
H	4.344	17.323	9.704
H	2.928	17.272	10.446
C	3.458	22.351	16.112
C	4.254	21.734	11.353
H	4.37	22.659	11.543
C	3.328	18.145	18.085
H	3.314	18.812	18.762
C	3.41	16.185	16.096
C	5.767	16.171	11.512
H	6.288	16.405	10.753
C	2.983	19.692	11.547
C	5.209	21.06	10.618
C	5.071	19.714	10.363
H	5.739	19.262	9.86
O	8.721	15.186	13.29
C	1.376	19.316	16.997
H	0.544	19.006	16.559
H	1.145	19.627	17.909
C	4.304	17.173	18.105
C	4.373	16.221	17.113
H	5.078	15.582	17.118

C	3.477	15.142	15.02
H	2.554	14.94	14.724
H	3.85	14.313	15.412
C	2.052	21.799	12.629
H	2.063	22.76	12.394
H	1.162	21.437	12.388
C	4.295	15.503	13.811
C	6.288	15.312	12.493
O	7.75	13.142	12.41
C	5.586	14.984	13.617
H	5.969	14.407	14.266
N	0.587	25.277	11.357
N	2.235	11.501	15.786
N	0.772	15.522	18.429
H	0.826	14.958	17.753
H	-0.074	15.603	18.669
N	2.061	21.273	8.625
H	2.422	20.473	8.746
H	1.802	21.589	9.41
N	0.048	19.657	21.18
C	1.908	25.528	11.333
H	2.282	26.109	11.985
N	4.032	17.484	6.191
C	0.544	25.544	14.756
H	1.044	26.347	14.664
C	3.002	22.116	8.051
C	0.569	24.853	15.96
H	1.121	25.168	16.667
C	3.367	12.399	17.649
H	4.17	12.498	18.147
C	-0.278	23.019	17.453
C	1.825	12.765	12.971
H	1.064	12.955	13.506
C	-0.198	23.71	16.15
C	1.845	18.169	21.383
H	2.743	18.011	21.65
C	2.203	12.975	18.123
C	2.086	13.54	11.854
H	1.506	14.259	11.634
C	2.662	11.714	13.319
C	0.815	23.844	9.474
H	0.413	23.256	8.844
C	4.008	24.305	7.794
H	4.04	25.224	8.035

C	2.217	13.789	19.357
C	4.074	12.217	11.444
H	4.848	12.019	10.931
C	-0.431	21.739	19.956
C	-0.204	25.077	13.69
C	3.956	20.181	6.786
C	0.695	22.454	19.607
H	1.422	22.514	20.216
C	1.098	17.116	20.822
C	-0.28	25.877	12.412
H	-1.217	25.902	12.094
H	0.01	26.806	12.587
C	0.046	24.45	10.426
H	-0.89	24.288	10.438
C	2.171	24.081	9.422
C	-0.923	23.208	15.038
H	-1.416	22.399	15.115
C	3.084	14.037	21.6
H	3.566	13.687	22.34
C	2.724	24.965	10.39
H	3.653	25.164	10.381
C	2.349	14.528	9.06
H	1.473	14.463	9.422
C	3.39	11.684	16.477
H	4.207	11.323	16.152
C	1.044	12.749	17.386
H	0.215	13.106	17.68
C	2.985	13.314	20.438
H	3.439	12.483	20.362
C	-1.4	22.318	17.826
H	-2.129	22.261	17.219
C	1.533	15.009	19.464
C	-0.906	23.898	13.842
H	-1.393	23.554	13.104
C	4.707	14.111	9.21
H	5.458	13.75	9.667
C	0.776	23.088	18.38
H	1.559	23.579	18.158
C	2.537	15.159	7.847
H	1.788	15.514	7.383
C	-0.225	17.413	20.472
H	-0.779	16.737	20.1
C	-1.502	21.685	19.062
H	-2.295	21.217	19.296

C	4.907	23.8	6.842
H	5.525	24.375	6.405
C	3.437	13.982	9.769
C	3.075	23.478	8.384
C	3.192	13.276	11.049
C	2.478	15.284	21.691
H	2.6	15.806	22.475
C	1.693	15.781	20.653
C	-0.515	21.024	21.276
H	-0.018	21.537	21.961
H	-1.462	20.97	21.561
C	5.136	18.104	6.565
H	5.945	17.61	6.624
C	3.782	11.493	12.58
H	4.385	10.812	12.856
C	2.862	18.164	6.049
H	2.082	17.711	5.751
C	2.288	10.795	14.459
H	1.402	10.393	14.272
H	2.948	10.059	14.511
C	-0.72	18.663	20.666
H	-1.623	18.845	20.435
C	4.878	22.465	6.558
H	5.512	22.106	5.95
C	1.311	19.403	21.548
H	1.838	20.096	21.928
C	4.897	14.763	7.981
H	5.771	14.848	7.622
C	3.815	15.282	7.291
C	3.945	21.63	7.137
C	5.144	19.436	6.869
H	5.952	19.857	7.136
C	1.102	12.004	16.231
H	0.303	11.849	15.742
C	4.014	16.016	5.984
H	4.869	15.731	5.575
H	3.282	15.78	5.361
C	2.811	19.509	6.344
H	1.993	19.984	6.245
N	7.76805	18.3818	14.31538
O	7.80805	17.5138	16.42038
C	6.53005	20.5458	14.34438
H	6.17405	21.3368	13.95338
C	7.42805	18.4198	15.64338



N	6.70405	19.3998	16.27338
C	7.41905	19.5608	13.48838
N	7.95505	19.3668	12.32938
H	8.41905	18.6368	12.17638
H	7.85605	19.9678	11.69338
C	6.31005	20.2818	15.50438
H	5.70005	20.8828	15.91238
O	8.59435	14.84216	15.95282
H	8.37549	15.65541	16.16483
H	8.61276	14.83891	15.08325
O	8.92293	17.29294	10.99325
H	9.03813	16.52528	10.59995
H	9.32302	17.91542	10.53398
H	6.51466	19.39991	17.25528

B3LYP/6-31G(d) Total Energy: -7068.2476726

**Complex 2 (1<sup>+</sup>·SC4<sup>+</sup>@5F-CTS)**

S	-0.54265	5.11188	3.03627
S	-5.49217	-0.46529	3.39135
S	5.24781	0.48606	3.25898
S	0.7477	-5.66244	3.56577
O	-0.34659	1.45188	-1.65537
H	0.50802	0.95034	-1.70963
O	-1.63111	4.59158	3.92247
O	-6.76008	0.07999	2.81445
O	1.81009	-0.17018	-1.55263
H	1.30161	-1.02345	-1.54037
O	-0.87833	6.45061	2.44958
O	-1.93153	-0.70809	-1.35474
H	-1.44844	0.14098	-1.53909
O	0.80406	5.08829	3.6795
O	0.19026	-2.28938	-1.27848
H	-0.67272	-1.80063	-1.35286
O	5.9972	1.75906	3.04414
O	6.12894	-0.72077	3.30932
O	-5.63623	-1.8503	3.92266
O	4.32042	0.57027	4.43915
O	-4.87932	0.49042	4.3798
C	-3.20044	0.62124	0.22439
O	2.15588	-5.48947	4.06135
C	-2.67069	-0.61601	-0.19299
C	0.85092	2.80471	-0.02825
C	-1.63468	3.42996	1.12806

H	-2.59136	3.66052	1.5864
C	3.09132	-1.20187	0.23378
C	1.56038	-3.22605	0.4108
C	-1.59535	2.57424	0.0265
C	0.77129	3.64991	1.08305
H	1.68383	4.06185	1.50134
C	0.26874	-2.97016	-0.08408
C	2.84384	1.23871	0.05766
C	-0.34528	2.2746	-0.54434
C	2.79404	-2.61928	-0.24544
H	3.65674	-3.24481	0.00148
H	2.69569	-2.63905	-1.33489
C	-0.45811	3.96477	1.65637
C	3.66981	1.38918	1.17216
H	3.90592	2.38705	1.52806
C	-4.03623	0.62939	1.34047
H	-4.47063	1.57081	1.66307
C	-2.91307	-1.80848	0.51144
C	1.68935	-4.01998	1.55125
H	2.67811	-4.24942	1.93381
C	2.57403	-0.06146	-0.40721
C	4.20557	0.27109	1.81268
C	3.90583	-1.01078	1.35462
H	4.32801	-1.87659	1.85411
O	-0.26043	-5.27559	4.60446
C	-2.8789	1.93197	-0.4847
H	-2.82717	1.77916	-1.56734
H	-3.70407	2.62714	-0.30439
C	-4.32955	-0.55075	2.02583
C	-3.75484	-1.75722	1.62976
H	-3.95755	-2.66494	2.18895
C	-2.30031	-3.13569	0.06941
H	-2.31343	-3.20298	-1.02408
H	-2.94828	-3.93711	0.43432
C	2.2197	2.46036	-0.60338
H	2.87999	3.31588	-0.4352
H	2.15675	2.31902	-1.68688
C	-0.88877	-3.41996	0.58234
C	0.55826	-4.50975	2.20356
O	0.50935	-7.02306	3.00394
C	-0.71796	-4.19146	1.73577
H	-1.59806	-4.53848	2.2673
N	4.40076	6.38382	-2.1837
N	-4.18909	-5.32705	-3.95157

N	-5.09234	-0.44733	-2.81182
H	-4.31524	-1.09134	-2.91198
H	-4.752	0.47872	-2.57668
N	5.35625	1.38725	-2.44498
H	4.97466	0.44743	-2.45225
H	4.60613	2.06957	-2.45158
N	-6.62824	4.24681	-1.70541
C	4.68725	6.16582	-0.87791
H	4.3235	6.90519	-0.17555
N	6.74169	-3.49372	-2.37481
C	1.39665	7.68547	-1.2974
H	1.92447	8.17156	-0.48114
C	6.35869	1.61363	-1.51561
C	0.0271	7.45179	-1.18736
H	-0.48763	7.76388	-0.2843
C	-5.21158	-4.50777	-1.96742
H	-5.43472	-4.66911	-0.91959
C	-2.15041	6.58717	-2.12273
C	-1.15794	-5.23376	-5.10567
H	-1.65467	-4.61951	-5.85245
C	-0.68976	6.84199	-2.23269
C	-6.9472	2.30729	-0.36576
H	-7.0788	1.8901	0.62562
C	-5.60933	-3.32379	-2.62101
C	0.2009	-5.05489	-4.86279
H	0.74043	-4.29014	-5.41315
C	-1.88991	-6.19136	-4.39172
C	5.51718	4.3693	-2.78164
H	5.8405	3.70882	-3.5765
C	7.59715	3.10717	-0.02597
H	7.77751	4.1102	0.34801
C	-6.40284	-2.30113	-1.9071
C	0.1343	-6.79722	-3.19757
H	0.62906	-7.4331	-2.46988
C	-4.92405	6.04914	-1.91926
C	2.09414	7.318	-2.45447
C	6.98432	-0.85195	-1.51297
C	-4.11408	6.06689	-0.77624
H	-4.55132	5.86734	0.19888
C	-6.86294	1.47397	-1.49751
C	3.57846	7.57408	-2.57467
H	3.85956	7.81369	-3.60054
H	3.89256	8.3924	-1.92581
C	4.81072	5.50394	-3.12611

H	4.56556	5.74681	-4.15219
C	5.83053	4.10363	-1.43443
C	0.02069	6.47461	-3.39068
H	-0.4964	5.98373	-4.2092
C	-8.24622	-1.84545	-0.37506
H	-9.04932	-2.20487	0.25929
C	5.39632	5.05117	-0.48487
H	5.59182	4.9113	0.5715
C	3.20125	-5.25751	-4.67305
H	2.83025	-5.15653	-5.68833
C	-4.50566	-5.4796	-2.64373
H	-4.16932	-6.39331	-2.16983
C	-5.258	-3.2021	-3.97963
H	-5.54711	-2.33471	-4.55961
C	-7.43488	-2.74029	-1.06328
H	-7.61671	-3.8068	-0.97295
C	-2.97523	6.58838	-3.2615
H	-2.55423	6.81911	-4.23511
C	-6.15299	-0.90463	-2.04741
C	1.38823	6.71132	-3.5009
H	1.91205	6.41976	-4.40768
C	2.85503	-5.79723	-2.34864
H	2.20275	-6.07448	-1.52635
C	-2.75032	6.32948	-0.87582
H	-2.14677	6.31609	0.02548
C	4.55381	-5.03867	-4.42033
H	5.21384	-4.75881	-5.2372
C	-6.67427	2.10735	-2.74224
H	-6.6305	1.53714	-3.66182
C	-4.33948	6.32063	-3.16159
H	-4.95603	6.33355	-4.05651
C	8.36493	2.05021	0.4478
H	9.13789	2.2189	1.18977
C	2.32281	-5.63018	-3.64024
C	6.60595	2.92078	-1.00296
C	0.87436	-5.83235	-3.90235
C	-8.02506	-0.48114	-0.53055
H	-8.66794	0.22832	-0.01872
C	-7.01084	0.00849	-1.36695
C	-6.39577	5.72296	-1.81549
H	-6.84901	6.17172	-0.9313
H	-6.94007	6.05951	-2.69902
C	6.81456	-3.22151	-1.05059
H	6.76423	-4.06921	-0.37899

C	-1.22776	-6.97204	-3.43733
H	-1.77689	-7.73171	-2.88728
C	6.7899	-2.48953	-3.28199
H	6.74016	-2.78039	-4.32355
C	-3.36885	-6.3731	-4.64128
H	-3.61011	-6.30001	-5.70255
H	-3.71808	-7.33655	-4.26896
C	-6.55991	3.47893	-2.81859
H	-6.41593	4.00125	-3.75632
C	8.13093	0.77327	-0.05211
H	8.72924	-0.06133	0.30064
C	-6.82225	3.67586	-0.49363
H	-6.86321	4.34687	0.35486
C	4.20809	-5.58047	-2.09735
H	4.59411	-5.70998	-1.08965
C	5.07138	-5.18632	-3.12763
C	7.15604	0.53642	-1.03149
C	6.94082	-1.92279	-0.60006
H	6.97973	-1.74473	0.46833
C	-4.55859	-4.20718	-4.61539
H	-4.28971	-4.1553	-5.66274
C	6.52811	-4.90223	-2.84484
H	6.92087	-5.54962	-2.06044
H	7.13854	-5.02578	-3.74025
C	6.90694	-1.17523	-2.88143
H	6.95915	-0.40788	-3.64399
N	-4.40543	-6.42973	4.38794
O	-6.59501	-5.78737	4.62543
C	-2.80551	-4.68525	3.94598
C	-5.39029	-5.49827	4.42368
N	-5.05928	-4.15768	4.25158
C	-3.13493	-6.06462	4.1606
N	-2.17904	-6.99788	4.13228
H	-2.42601	-7.96262	4.3859
H	-1.19227	-6.75209	4.0418
C	-3.78222	-3.75156	4.00138
H	-3.60052	-2.69027	3.87653
H	-5.83777	-3.48585	4.22181
F	-1.51472	-4.345	3.70366

B3LYP/6-31G(d) Total Energy: -7014.5890289

#### S14. HPLC analyses of CTS and 5F-CTS in the precipitate and supernatant in *n*-butanol

CTS (10 mg) and 5F-CTS (10 mg) were added to *n*-butanol, dissolved as much as possible by ultrasound and heating. The precipitate was filtered. Both the supernatant and the precipitate were dissolved separately by methanol. After filtration with membranes (0.22  $\mu\text{m}$ ), aliquot of each solution (10  $\mu\text{L}$ ) was injected for HPLC analysis (HPLC conditions: column: Ultimate Polar-RP column (250  $\times$  4.6 mm, 5  $\mu\text{m}$ ), mobile phase: 0.1% formic acid in water (A) MeOH (B); gradient profiles:98% B; flow rate: 1.0 mL/min, detection: UV at 280 nm). The results showed that both CTS and 5F-CTS were present in the precipitate and supernatant, and *n*-butanol could not separate CTS and 5F-CTS.

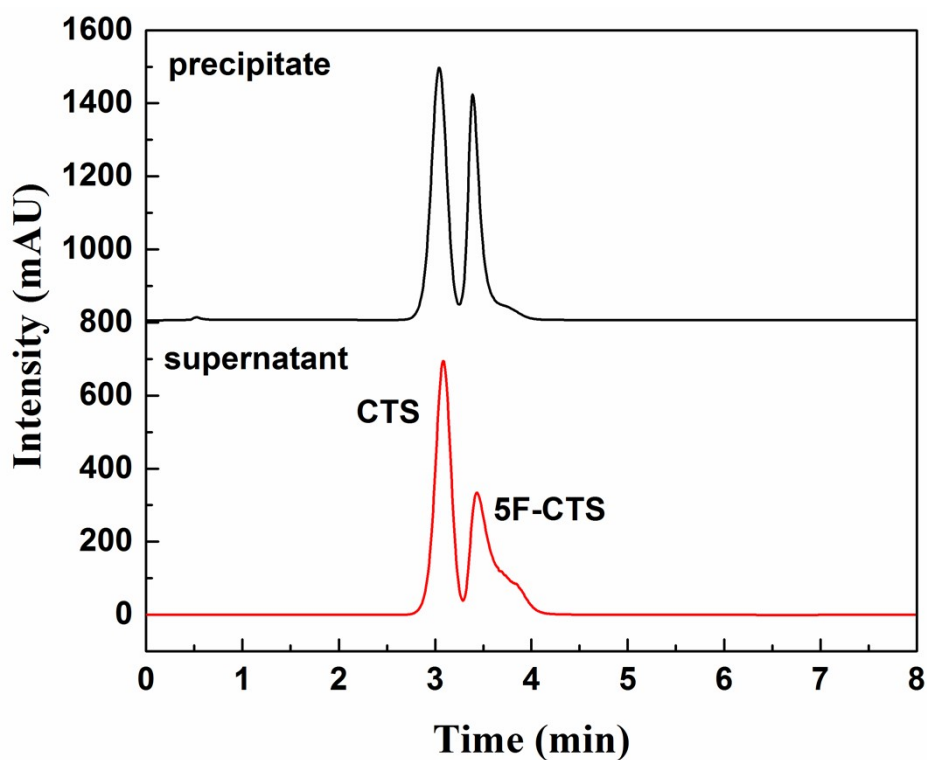


Figure S14. HPLC chromatograms of CTS and 5F-CTS in the precipitate and supernatant fractions in *n*-butanol.

Table S1. Experimental single crystal X-ray data of  $1^{4+}\cdot\text{SC4}^4$ ,  $1^{4+}\cdot\text{SC4}^4\text{@CTS}$  and  $1^{4+}\cdot\text{SC4}^4\text{@5F-CTS}$ .

Items	$1^{4+}\cdot\text{SC4}^4$	$1^{4+}\cdot\text{SC4}^4\text{@CTS}$	$1^{4+}\cdot\text{SC4}^4\text{@5F-CTS}$
Formula	$\text{C}_{60}\text{H}_{50}\text{N}_6$ , $\text{C}_{28}\text{H}_{21}\text{O}_{16}\text{S}_4$	$\text{C}_{60}\text{H}_{50}\text{N}_6$ , $\text{C}_{28}\text{H}_{21}\text{O}_{16}\text{S}_4$ , $\text{C}_4\text{H}_5\text{N}_3\text{O}$ , 18( $\text{H}_2\text{O}$ )	1.75( $\text{C}_{60}\text{H}_{50}\text{N}_6$ ), 2( $\text{C}_{28}\text{H}_{21}\text{O}_{16}\text{S}_4$ ), 3( $\text{C}_4\text{H}_4\text{FN}_3\text{O}$ )
$M_w$ [gmol <sup>-1</sup> ]	1596.74	2031.13	3365.01
System	orthorhombic	monoclinic	triclinic
Space group	<i>Pbca</i>	<i>P2</i> <sub>1</sub>	<i>P1</i>
a(Å)	18.1619(2)	9.6436(2)	17.5343(2)
b(Å)	18.4892(2)	27.2935(6)	18.0124(2)
c(Å)	54.2241(9)	18.6722(4)	38.1267(3)
α(°)	90	90	84.4770(10)
β(°)	90	104.207(2)	79.2180(10)
γ(°)	90	90	66.3020(10)
V(Å <sup>3</sup> )	18208.4(4)	4764.35(18)	10828.7(2)
Z	8	2	2
$d_{\text{calcd}}$ [Mg/cm <sup>3</sup> ]	1.165	1.416	1.032
R <sub>int</sub>	0.0681	0.0710	0.0318
GOOF	1.042	1.090	1.785
Flack	-	0.040(15)	-
Temperature (K)	100.00(10)	100.00(10)	100.00(10)
R <sub>1</sub> [I > 2σ(I)]	0.0738	0.0760	0.1251
wR <sub>2</sub> (all data)	0.2310	0.2094	0.4141
F(000)	6664.0	2140.0	3498.0
CCDC No.	2253871	2253872	2253873

Table S2. Aromatic intermolecular interactions in Host and Guest

Table S2a. C—H $\cdots\pi$  intermolecular interactions in Host and Guest

Host-Guest	X-H $\cdots$ Cg	H $\cdots$ Cg(Å)	X-H $\cdots$ Cg(°)	X $\cdots$ Cg(Å)
<b>1<sup>4+</sup>.SC4<sup>4-</sup></b>	C <sub>17</sub> -H <sub>17</sub> A $\cdots$ Cg2 <sup>a</sup>	2.67	128	3.380(4)
	C <sub>47</sub> -H <sub>47</sub> A $\cdots$ Cg1 <sup>b</sup>	2.85	132	3.593(4)
	C <sub>67</sub> -H <sub>67</sub> B $\cdots$ Cg3	2.87	124	3.513(4)
	C <sub>81</sub> -H <sub>81</sub> A $\cdots$ Cg2	2.87	128	3.564(4)

Symmetry codes: <sup>a</sup> 1+X,Y,Z; <sup>b</sup> -1+X,Y,Z; Cg1 is the centroid of N2, C14, C13, C12, C16 and C15; Cg2 is the centroid of N4, C44, C43, C42, C46 and C45; Cg3 is the centroid of C18, C19, C20, C21, C22 and C23;

Host-Guest	X-H $\cdots$ Cg	H $\cdots$ Cg(Å)	X-H $\cdots$ Cg(°)	X $\cdots$ Cg(Å)
<b>1<sup>4+</sup>.SC4<sup>4-</sup>@CTS</b>	N <sub>5</sub> -H <sub>5</sub> A $\cdots$ Cg12	2.89	112	3.324(1)
	N <sub>6</sub> -H <sub>6</sub> A $\cdots$ Cg14	2.98	107	3.348(1)
	C <sub>67</sub> -H <sub>67</sub> A $\cdots$ Cg1	2.86	145	3.712(1)
	C <sub>74</sub> -H <sub>74</sub> A $\cdots$ Cg6	3.00	115	3.534(1)
	S <sub>3</sub> -O <sub>8</sub> $\cdots$ Cg5	3.36	104	3.944(1)

Symmetry codes: Cg1 is the centroid of N1, C2, C1, C5, C4 and C3; Cg5 is the centroid of C6, C7, C8, C9, C10 and C11; Cg6 is the centroid of C18, C19, C20, C21, C22 and C23; Cg12 is the centroid of C68, C69, C70, C71, C72 and C73; Cg14 is the centroid of C82, C83, C84, C85, C86 and C87.

Host-Guest	X-H $\cdots$ Cg	H $\cdots$ Cg(Å)	X-H $\cdots$ Cg(°)	X $\cdots$ Cg(Å)
<b>1<sup>4+</sup>.SC4<sup>4-</sup>@5F-CTS</b>	C <sub>116</sub> -H <sub>11</sub> B $\cdots$ Cg6	2.85	135	3.614(8)
	C <sub>125</sub> -H <sub>125</sub> $\cdots$ Cg19	2.74	162	3.651(12)
	C <sub>127</sub> -H <sub>127</sub> $\cdots$ Cg17	2.64	156	3.528(14)
	C <sub>135</sub> -H <sub>135</sub> $\cdots$ Cg25	2.85	131	3.544(15)
	C <sub>156</sub> -H <sub>156</sub> $\cdots$ Cg22	2.57	167	3.506(5)
	C <sub>157</sub> -H <sub>157</sub> $\cdots$ Cg23	2.93	98	3.196(5)
	C <sub>158</sub> -H <sub>158</sub> $\cdots$ Cg20	2.61	155	3.495(5)
	S <sub>2</sub> -O <sub>4</sub> $\cdots$ Cg24	3.10	130	4.148(4)
	S <sub>4</sub> -O <sub>12</sub> $\cdots$ Cg25	3.09	115	3.897(5)
S <sub>7</sub> -O <sub>23</sub> $\cdots$ Cg12	3.15	118	4.035(2)	

Symmetry codes: Cg6 is the centroid of C18, C19, C20, C21, C22 and C23; Cg12 is the centroid of N11, C161, C160, C159, C163 and C162; Cg17 is the centroid of C68, C69, C70, C71, C72 and C73; Cg19 is the centroid of C82, C83, C84, C85, C86 and C87; Cg20 is the centroid of C89, C90, C91, C92, C93 and C94; Cg22 is the centroid



of C103, C104, C105, C106, C107 and C108; Cg23 is the centroid of C110, C111, C112, C113, C114 and C115; Cg24 is the centroid of N7, C117, C118, C119, C120 and C121; Cg25 is the centroid of N8, C130, C129, C128, C132 and C131.

Table S2b.  $\pi \cdots \pi$  intermolecular interactions in Host and Guest

Host-Guest	Cg $\cdots$ Cg	Cg $\cdots$ Cg(Å)	Cg $\cdots$ Cg(°)
<b>1<sup>4+</sup>·SC4<sup>4-</sup></b>	Cg3 $\cdots$ Cg6 <sup>a</sup>	3.63	2.14

Symmetry codes: <sup>a</sup> -1/2+X,1/2-Y,1-Z; Cg3 is the centroid of C18, C19, C20, C21, C22 and C23; Cg6 is the centroid of C18, C19, C20, C21, C22 and C23.

Host-Guest	Cg $\cdots$ Cg	Cg $\cdots$ Cg(Å)	Cg $\cdots$ Cg(°)
<b>1<sup>4+</sup>·SC4<sup>4-</sup>@5F-CTS</b>	Cg10 $\cdots$ Cg29 <sup>a</sup>	3.86	13.8

Symmetry codes: <sup>a</sup> X,Y,Z; Cg10 is the centroid of C54, C55, C56, C57, C58 and C59; Cg29 is the centroid of N2A, C2A, C1A, C4A, N3A and C3A.

Table S3. Hydrogen bonding intermolecular interactions in Host and Guest

H-G	Interactions	D-H (Å)	D...A (Å)	H...A (Å)	D-H...A (deg)	Symmetry code
<b>1<sup>4+</sup>·SC4<sup>4+</sup></b>	C <sub>9</sub> -H <sub>9</sub> ...O <sub>11</sub>	0.95	2.45	3.349(5)	158	3/2-x,-1/2+y,z
	C <sub>14</sub> -H <sub>14</sub> ...O <sub>8</sub>	0.95	2.22	3.117(6)	157	3/2-x,-1/2+y,z
	C <sub>26</sub> -H <sub>26</sub> ...O <sub>6</sub>	0.95	2.48	3.297(5)	144	1/2-x,-1/2+y,z
	C <sub>31</sub> -H <sub>31</sub> ...O <sub>9</sub>	0.95	2.34	3.275(5)	168	1-x,1-y,1-z
	C <sub>46</sub> -H <sub>46</sub> ...O <sub>7</sub>	0.95	2.45	3.283(5)	146	1/2-x,-1/2+y,z
	C <sub>50</sub> -H <sub>50</sub> ...O <sub>1</sub>	0.95	2.41	3.331(7)	163	1/2-x,-1/2+y,z
	C <sub>59</sub> -H <sub>59</sub> ...O <sub>2</sub>	0.95	2.59	3.523(9)	166	1/2-x,-1/2+y,z
<b>1<sup>4+</sup>·SC4<sup>4+</sup> @CTS</b>	N <sub>2</sub> A-H <sub>2</sub> AB...O <sub>9</sub>	0.88	2.06	2.896(1)	159	1+x,y,z
	C <sub>13</sub> -H <sub>13</sub> ...O <sub>7</sub>	0.95	2.51	3.350(1)	147	x,y,z
	C <sub>43</sub> -H <sub>43</sub> ...O <sub>2</sub>	0.95	2.53	3.266(1)	134	x,y,z
	C <sub>45</sub> -H <sub>45</sub> ...O <sub>1</sub>	0.95	2.26	3.084(1)	145	1+x,y,z
	C <sub>50</sub> -H <sub>50</sub> ...O <sub>11</sub>	0.95	2.57	3.516(1)	172	x,y,z
<b>1<sup>4+</sup>·SC4<sup>4+</sup> @5F-CTS</b>	N <sub>1</sub> A-H <sub>1</sub> AA...O <sub>1</sub> B	0.88	1.87	2.742(5)	169	x,y,z
	N <sub>3</sub> B-H <sub>3</sub> BA...O <sub>1</sub> A	0.88	2.16	2.993(5)	158	x,y,z
	N <sub>3</sub> B-H <sub>3</sub> BB...O <sub>1</sub> C	0.88	2.13	2.930(5)	151	x,y,z
	N <sub>3</sub> B-H <sub>3</sub> BB...N <sub>1</sub> C	0.88	2.61	2.974(7)	106	x,y,z
	N <sub>3</sub> C-H <sub>3</sub> CA...O <sub>1</sub> A	0.88	2.19	3.002(7)	153	x,y,z
	O <sub>13</sub> -H <sub>13</sub> A...O <sub>29</sub>	0.88	2.57	3.306(5)	116	x,y,z
	O <sub>15</sub> -H <sub>15</sub> A...O <sub>30</sub>	0.84	1.84	2.564(6)	143	x,y,z
	C <sub>116</sub> -H <sub>11</sub> A...O <sub>13</sub>	0.99	2.51	3.446(7)	157	x,y,z
	C <sub>164</sub> -H <sub>16</sub> B...F <sub>1</sub> C	0.99	2.47	3.330(6)	145	-1-x,-y,1-z
	C <sub>34</sub> -H <sub>34</sub> ...O <sub>5</sub>	0.95	2.42	3.355(10)	169	x,y,z
	C <sub>67</sub> -H <sub>67</sub> B...O <sub>32</sub>	0.99	2.40	3.314(7)	153	x,y,z
	C <sub>74</sub> -H <sub>74</sub> B...O <sub>30</sub>	0.99	2.41	3.376(7)	165	x,y,z
	C <sub>95</sub> -H <sub>95</sub> B...O <sub>15</sub>	0.99	2.53	3.478(7)	160	x,y,z
	C <sub>129</sub> -H <sub>129</sub> ...O <sub>1</sub>	0.95	2.52	3.24(2)	133	x,y,z
	C <sub>144</sub> -H <sub>144</sub> ...O <sub>2</sub>	0.95	2.54	3.347(19)	143	1+x,y,z
C <sub>144</sub> -H <sub>144</sub> ...O <sub>3</sub>	0.95	2.56	3.42(2)	151	1+x,y,z	

Table S4 <sup>1</sup>H-NMR shift changes after formation of **1<sup>4+</sup>·SC4<sup>4-</sup>**

	<b>SC4H</b>	<b>1·(PF<sub>6</sub>)<sub>4</sub></b>	<b>1<sup>4+</sup>·SC4<sup>4-</sup></b>	<b>Δppm</b>
<b>H1</b>	7.372	-	7.306	-0.066
<b>H2</b>	3.930	-	3.843	-0.087
<b>Ha</b>		6.944	6.919	-0.025
<b>Hb</b>		7.366	7.347	-0.019
<b>Hc</b>		8.249	8.233	-0.016
<b>Hd</b>		9.270	9.222	-0.048
<b>He</b>		5.866	5.856	-0.01
<b>Hf, Hg</b>		7.761	7.733	-0.028

Table S5. <sup>1</sup>H-NMR shift changes after the formation of ternary complex **1<sup>4+</sup>·SC4<sup>4-</sup>@CTS**

	<b>CTS</b>	<b>SC4H</b>	<b>1·(PF<sub>6</sub>)<sub>4</sub></b>	<b>1<sup>4+</sup>·SC4<sup>4-</sup>@CTS</b>	<b>Δppm</b>
<b>H1</b>	-	7.372	-	8.156	0.784
<b>H2</b>	-	3.930	-	-	-
<b>Ha</b>	-	-	6.944	6.942	-0.002
<b>Hb</b>	-	-	7.366	7.364	-0.002
<b>Hc</b>	-	-	8.249	8.246	-0.003
<b>Hd</b>	-	-	9.270	9.245	-0.025
<b>He</b>	-	-	5.866	5.847	-0.019
<b>Hf, Hg</b>	-	-	7.761	7.748	-0.013
<b>HA</b>	10.416	-	-	12.032	1.616
<b>HB</b>	7.035	-	-	-	-
<b>HC</b>	5.576	-	-	5.930	0.354
<b>HD</b>	7.320	-	-	9.415	2.095

Table S6.  $^1\text{H}$ -NMR shift changes after the formation of ternary complex  $1^{4+}\cdot\text{SC4}^{4-}$   
@5F-CTS

	CTS	SC4H	$1\cdot(\text{PF}_6)_4$	$1^{4+}\cdot\text{SC4}^{4-}$ @CTS	$\Delta\text{ppm}$
<b>H1</b>	-	7.372	-	8.176	0.376
<b>H2</b>	-	3.930	-	-	-
<b>Ha</b>	-	-	6.944	6.942	-0.002
<b>Hb</b>	-	-	7.366	7.364	-0.002
<b>Hc</b>	-	-	8.249	8.247	-0.002
<b>Hd</b>	-	-	9.270	9.245	-0.025
<b>He</b>	-	-	5.866	5.847	-0.019
<b>Hf, Hg</b>	-	-	7.761	7.748	-0.013
<b>HA</b>	10.226	-	-	9.541	-0.725
<b>HB</b>	7.336	-	-	-	-
<b>HC</b>	7.600	-	-	8.793	1.193

## References

- s1. Frisch, M. J.; Trucks, G. W.; Schlegel, H. B.; Scuseria, G. E.; Robb, M. A.; Cheeseman, J. R.; Scalmani, G.; Barone, V.; Petersson, G. A.; Nakatsuji, H.; Li, X.; Caricato, M.; Marenich, A. V.; Bloino, J.; Janesko, B. G.; Gomperts, R.; Mennucci, B.; Hratchian, H. P.; Ortiz, J. V.; Izmaylov, A. F.; Sonnenberg, J. L.; Williams-Young, D.; Ding F.; Lipparini, F.; Egidi, F.; Goings, J.; Peng, B.; Petrone, A.; Henderson, T.; Ranasinghe, D.; Zakrzewski, V. G.; Gao, J.; Rega, N.; Zheng, G.; Liang, W.; Hada, M.; Ehara, M.; Toyota, K.; Fukuda, R.; Hasegawa, J.; Ishida, M.; Nakajima, T.; Honda, Y.; Kitao, O.; Nakai, H.; Vreven, T.; Throssell, K.; Montgomery, J. A. Jr.; Peralta, J. E.; Ogliaro, F.; Bearpark, M. J.; Heyd, J. J.; Brothers, E. N.; Kudin, K. N.; Staroverov, V. N.; Keith, T. A.; Kobayashi, R.; Normand, J.; Raghavachari, K.; Rendell, A. P.; Burant, J. C.; Iyengar, S. S.; Tomasi, J.; Cossi, M.; Millam, J. M.; Klene, M.; Adamo, C.; Cammi, R.; Ochterski, J. W.;

Martin, R. L.; Morokuma, K.; Farkas, O.; Foresman, J. B.; Fox, D. J. *Gaussian 16*, Gaussian, Inc., Wallingford CT, **2016**.

- s2. Becke, A. D. Density-functional theory vs density-functional fits: The best of both. *J. Chem. Phys.* **2022**, *157*, 234102.
- s3. Marenich, A. V.; Cramer, C. J.; Truhlar, D. G. Universal solvation model based on solute electron density and on a continuum model of the solvent defined by the bulk dielectric constant and atomic surface tensions. *J. Phys. Chem. B* **2009**, *113*, 6378-96.